

Millimeter Wave Communications With Reconfigurable Intelligent Surface: Performance Analysis and Optimization

Hongyang Du, Jiayi Zhang, *Member, IEEE*, Julian Cheng, *Senior Member, IEEE*,
Zhaohu Lu, and Bo Ai, *Senior Member, IEEE*

Abstract

Reconfigurable Intelligent Surface (RIS) can create favorable multipath to establish strong links that are useful in millimeter wave (mmWave) communications. While previous works used Rayleigh or Rician fading, we use the fluctuating two-ray (FTR) distribution to model the small-scale fading in mmWave frequency. First, we obtain the statistical characterizations of the product of independent FTR random variables (RVs) and the sum of product of FTR RVs. For the RIS-aided and amplify-and-forward (AF) relay systems, we derive exact end-to-end signal-to-noise ratio (SNR) expressions. To maximize the end-to-end SNR, we propose a novel and simple way to obtain the optimal phase shifts at the RIS elements. The optimal power allocation scheme for the AF relay system is also proposed. Furthermore, we evaluate important performance metrics including the outage probability and the average bit error probability. To validate the accuracy of our analytical results, Monte-Carlo simulations are subsequently conducted to provide interesting insights. It is found that the RIS-aided system can achieve the same performance as the AF relay system with low transmit power. More interestingly, as the channel conditions improve, the RIS-aided system can outperform the AF relay system having the same transmit power with a smaller number of reflecting elements.

Index Terms

Fluctuating two-ray, mmWave communications, phase shift, reconfigurable intelligent surface.

H. Du and J. Zhang are with the School of Electronic and Information Engineering, Beijing Jiaotong University, Beijing 100044, China. (e-mail: {17211140; jiayizhang}@bjtu.edu.cn)

J. Cheng is with the School of Engineering, The University of British Columbia, Kelowna, BC V1V 1V7, Canada. (e-mail: julian.cheng@ubc.ca).

Z. Lu is with the Algorithm Department, Wireless Product Research and Development Institute, Wireless Product Operation, ZTE Corporation, Shenzhen 518000, China. (e-mail: lu.zhaohua@zte.com.cn).

B. Ai is with the State Key Laboratory of Rail Traffic Control and Safety, Beijing Jiaotong University, Beijing 100044, China. (e-mail: boai@bjtu.edu.cn)

I. INTRODUCTION

As a promising technique for supporting skyrocket data rate in the fifth-generation (5G) cellular networks, millimeter wave (mmWave) communications have received an increasing attention due to the large available bandwidth at mmWave frequencies [1]. In recent years, research on channel modeling for mmWave wireless communications has been intense both in industry and academia [2], [3]. Based on recent small-scale fading measurements of the 28 GHz outdoor millimeter-wave channels [3], the fluctuating two-ray (FTR) fading model has been proposed as a versatile model that can provide a much better fit than the legacy Rician fading model.

However, one of the fundamental challenges of mmWave communication is the susceptibility to blockage effects. Thus, hindrances still occur due to the existence of buildings, trees, cars, and even human body. To address this problem, a typical solution is to add new supplementary links. For example, the amplify-and-forward (AF) relay can be introduced in areas to receive the weak signal and then amplify and re-transmit it toward the destination [4]. Alternatively, reconfigurable intelligent surfaces (RISs), comprised of many reflecting elements, have recently drawn significant attention due to their superior capability in manipulating electromagnetic waves [5]. Taking advantage of cheap and nearly passive RIS attached in facades of buildings, signals from the base station (BS) can be re-transmitted along desired directions by tuning their phases shifts, thereby leveraging the line-of-sight (LoS) components between the RIS and users to maintain good communication quality.

Obviously, RIS and relay operate in different mechanisms to provide supplementary links. With the help of RIS, the propagation environment can be improved because of extremely low power consumption without introducing additional noise, but the incident signal at the reflector array is reflected without being amplified. Thus, whether the RIS is more economical and efficient than the relay is still controversial. In [6], a comparison between RIS and an ideal full-duplex relay was made and it was found that large energy efficiency gains by using an RIS, but the setup is not representative for a typical relay. Besides, authors in [7] made a fair comparison between RIS-aided transmission and conventional decode-and-forward (DF) relaying, with the purpose of determining how large an RIS needs to be to outperform conventional relaying, and it is found that a large number of reflecting elements are needed to outperform the DF relaying in terms of minimizing the total transmit power and maximizing the energy efficiency. However, previous works did not build on a versatile statistical channel model that well characterizes wireless propagation in mmWave communications to derive performance metrics.

In this paper, we aim to answer the significant question “*How can a RIS outperform AF relaying over realistic mmWave channels?*”. Using the FTR fading channel model, we derive novel exact expressions to analyze the system performance for both systems. The main contributions of this paper are summarized as follows:

- First, we derive the exact probability density function (PDF), cumulative distribution function (CDF), and generalized moment generating function of a product of independent but not identically distributed (i.n.i.d.) FTR random variables (RVs) and the sum of product of FTR RVs. These statistical characteristics are useful in many communication scenarios, such as multi-hop wireless communication systems [8] and keyhole channels of multiple-input multiple-output (MIMO) systems [9].
- To provide a fair comparison between RIS-aided transmission and AF relaying, we propose an optimal power allocation scheme for AF relay systems, and we further use a binary search tree method to obtain optimal phases at the RIS. Besides, the convergence of the proposed phase optimization method is investigated.
- We derive a novel generic single integral expression for the CDF of the end-to-end signal-to-noise ratio (SNR) of AF systems by considering not identically distributed hops and hardware impairments. For the cases of non-ideal and ideal hardware, we obtain the exact PDF and CDF expressions of the end-to-end SNR.
- Assuming ideal transceiver hardware, we provide a fair comparison between RIS-aided system and AF relay aided communication system. The exact outage probability (OP) and average bit error probability (ABEP) expressions are derived for both scenarios to obtain important engineering insights. It is interesting to find that the RIS-aided system can achieve the same OP and ABEP as the AF relay system with less reflecting elements if the transmit power is low. More importantly, as the channel conditions improve, the RIS-aided system achieves more ABEP reduction than the AF relay aided system having the same transmit power.

The remainder of the paper is organized as follows. In Section II, we briefly introduce the RIS-aided and AF relay systems, and derive exact statistics for the end-to-end SNR of both systems. Section III presents the optimal phase shift of the RIS’s reflector array and the optimal power allocation scheme for the AF relay system. Performance metrics of two systems, such as OP and ABEP, are carried out in Section IV. In Section V, numerical results accompanied with Monte-Carlo simulations are presented. Finally, Section VI concludes this paper.

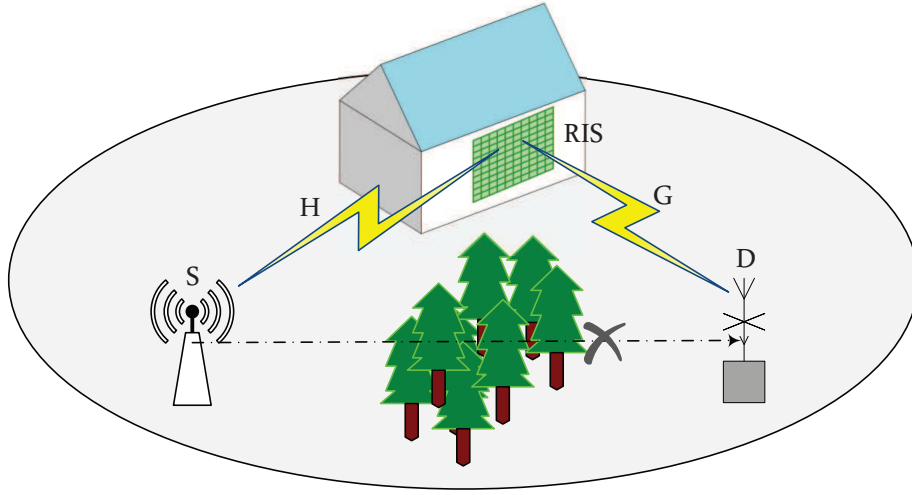


Fig. 1. Intelligent reflecting surface supported transmission.

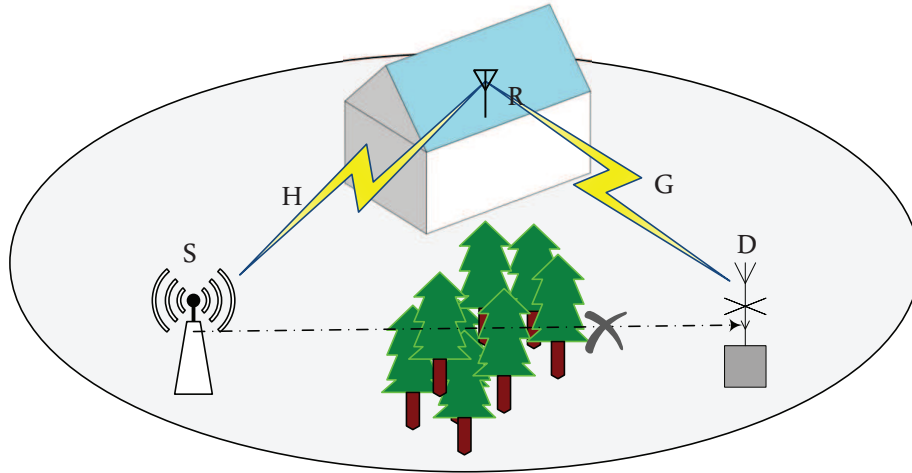


Fig. 2. Relay supported transmission

II. SYSTEM MODEL AND PRELIMINARIES

A. System Description

We focus on a single cell of a mmWave wireless communication system and analyze two scenarios: when RIS is adopted and when AF relay is used, as shown in Fig. 1 and Fig. 2 respectively. To characterize the performance of the considered mmWave communication system, we assume that the global channel state information (CSI) is perfectly known at the BS, RIS and relay.¹ In Fig. 1, the RIS is set up between the BS and the user, comprising L reflector elements arranged in a uniform array. In addition, the reflector elements are configurable and programmable via an RIS controller. In Fig. 2, a half-duplex AF relay is

¹An efficient CSI acquisition method for RIS-aided mmWave networks has been proposed [10]. Besides, the results in this paper serve as theoretical performance upper bounds for the considered system.

deployed at the same location as the RIS.² We consider the classic repetition coded AF relaying protocol [11] where the transmission is divided into two equal phases.

More specifically, we assume that the direct transmission link between the BS and the user is blocked by trees or buildings. Thus, the RIS or relay is deployed to leverage the LoS paths to enhance the quality of received signals. In addition, the fluctuating two-ray (FTR) fading model has been proposed in [3] as a generalization of the two-wave with diffuse power fading model. The FTR fading model allows the constant amplitude specular waves of LoS propagation to fluctuate randomly, and incorporates ground reflections to provide a much better fit for small-scale fading measurements in mmWave communications [12]. In the following, we use the FTR fading model to illustrate the mmWave links.

B. Exact Statistics of the End-to-End SNR For RIS-aided System

In this subsection, we present some useful statistical expressions which are useful for the performance analysis of RIS-aided system.

1) *Exact PDF and CDF of the Product of FTR RVs:* The PDF and CDF of the squared FTR RV γ are given respectively as [12]

$$f_{\gamma}(\gamma) = \frac{m^m}{\Gamma(m)} \sum_{j=0}^{\infty} \frac{K^j d_j}{j!} f_G(\gamma; j+1, 2\sigma^2), \quad (1)$$

$$F_{\gamma}(\gamma) = \frac{m^m}{\Gamma(m)} \sum_{j=0}^{\infty} \frac{K^j d_j}{j!} F_G(\gamma; j+1, 2\sigma^2) \quad (2)$$

where

$$f_G(\gamma; j+1, 2\sigma^2) = \frac{\gamma^j}{\Gamma(j+1)(2\sigma^2)^{j+1}} \exp\left(-\frac{\gamma}{2\sigma^2}\right), \quad (3)$$

$$F_G(x; j+1, 2\sigma^2) \triangleq \frac{1}{\Gamma(j+1)} \gamma\left(j+1, \frac{x}{2\sigma^2}\right), \quad (4)$$

and

$$d_n \triangleq \sum_{k=0}^n \binom{n}{k} \left(\frac{\Delta}{2}\right)^k \sum_{l=0}^k \binom{k}{l} \Gamma(n+m+2l-k) e^{\frac{\pi(2l-k)j}{2}} \times ((m+K)^2 - (K\Delta)^2)^{\frac{-(n+m)}{2}} P_{n+m-1}^{k-2l} \left(\frac{m+K}{\sqrt{(m+K)^2 - (K\Delta)^2}} \right) \quad (5)$$

²The RIS-aided system has been compared with the classic DF relaying in deterministic flat-fading channel where all channel gains have the same squared magnitude [7].

where $\gamma(\cdot, \cdot)$ is the incomplete gamma function [13, eq. (8.350.1)], $P(\cdot)$ is the Legendre function of the first kind [13, eq. (8.702)], K denotes the average power ratio of the dominant wave to the scattering multipath, m is the fading severity parameter, and Δ is a parameter varying from 0 to 1 representing the similarity of two dominant waves. In addition, the received average SNR is given by $\nu = \mathbb{E}[|V_r|^2] = 2\sigma^2(1 + K)$.

Substituting $R = \sqrt{\gamma}$ into (1), we can easily obtain the PDF expression of FTR RVs. Thus, let $X \triangleq \prod_{\ell=1}^N R_\ell$ as the product of N FTR RVs, where $R \sim \mathcal{FTR}(K_\ell, m_\ell, \Delta_\ell, \sigma_\ell^2)$ ($\ell = 1, \dots, N$), we can derive the exact s_{th} moment, PDF and CDF expressions for X , which are summarized in the following Theorems.

Theorem 1. *The s th moment of X is given by*

$$\mathbb{E}[X^s] = \prod_{\ell=1}^N \frac{m_\ell^{m_\ell}}{\Gamma(m_\ell)} \sum_{j_\ell=0}^{\infty} \frac{K_\ell^{j_\ell} d_{\ell j_\ell}}{j_\ell!} \frac{(2\sigma_\ell^2)^{\frac{s}{2}}}{\Gamma(j_\ell + 1)} \Gamma\left(1 + j_\ell + \frac{s}{2}\right). \quad (6)$$

Proof: The s th order moment of X around the origin is derived as

$$\mathbb{E}[X^s] = \prod_{\ell=1}^N \mathbb{E}[R_\ell^s] = \prod_{\ell=1}^N \int_0^\infty r^s f_{R_\ell}(r) dr. \quad (7)$$

By substituting (1) into (7) and using [13, eq. (3.381.10)] and [13, eq. (8.356.3)], we obtain the s th moment of X , which completes the proof. ■

Theorem 2. *The PDF, CDF and MGF expressions of X can be deduced in closed-form as*

$$f_X(x) = \sum_{j_1, \dots, j_N=0}^{\infty} \prod_{\ell=1}^N \frac{m_\ell^{m_\ell}}{\Gamma(m_\ell)} \frac{2x^{-1}}{\Gamma(j_\ell + 1)} \frac{K_\ell^{j_\ell} d_{\ell j_\ell}}{j_\ell!} G_{0,N}^{N,0} \left(x^2 \prod_{\ell=1}^N \left(\frac{1}{2\sigma_\ell^2} \right) \middle| \begin{matrix} - \\ 1 + j_1, \dots, 1 + j_N \end{matrix} \right), \quad (8)$$

$$F_X(x) = \sum_{j_1, \dots, j_N=0}^{\infty} \prod_{\ell=1}^N \frac{m_\ell^{m_\ell}}{\Gamma(m_\ell)} \frac{1}{\Gamma(j_\ell + 1)} \frac{K_\ell^{j_\ell} d_{\ell j_\ell}}{j_\ell!} G_{1,N+1}^{N,1} \left(x^2 \prod_{\ell=1}^N \left(\frac{1}{2\sigma_\ell^2} \right) \middle| \begin{matrix} 1 \\ 1 + j_1, \dots, 1 + j_N, 0 \end{matrix} \right), \quad (9)$$

$$\mathcal{M}_X(s) = \sum_{j_1, \dots, j_N=0}^{\infty} \prod_{\ell=1}^N \frac{K_\ell^{j_\ell} d_{\ell j_\ell}}{j_\ell!} \frac{m_\ell^{m_\ell}}{\Gamma(m_\ell)} \frac{1}{\Gamma(j_\ell + 1)} H_{1,1}^{1,1} \left(\frac{1}{s \prod_{\ell=1}^N (\sqrt{2}\sigma_\ell)} \middle| \begin{matrix} (1, 1) \\ (1 + j_\ell, 0.5) \end{matrix} \right) \quad (10)$$

where $G_{p,q}^{m,n}(\cdot)$ is the Meijer's G -function [13, eq. (9.301)] and $H_{p,q}^{m,n}(\cdot)$ is the Fox's H -function [14, eq. (1.2)].

Proof: Please refer to Appendix A. ■

Remark 1. Although the PDF, CDF and MGF of a product of N i.n.i.d. squared FTR RVs have been respectively derived in [15, eq. (7)], [15, eq. (16)] and [15, eq. (17)]. Only the parameter m of each FTR RV is different from each other. In the practical mmWave communication scenario, all parameters K, m, Δ and σ^2 of each FTR RV can be different, thus the statistical characterizes obtained in Theorem 2 are more general and useful in the performance analysis.

Remark 2. Substituting $\gamma = x^2$ into (8) and (9), we can obtain more general statistical expressions of the product of an arbitrary number of i.n.i.d. squared FTR RVs. Besides, note that the bivariate Meijer's G -function can be evaluated numerically in an efficient manner using the MATLAB program [16], and two Mathematica implementations of the single Fox's H -function are provided in [17] and [18].

2) *Exact PDF and CDF of the Sum of Product of FTR RVs:* We derive the exact PDF and CDF of the sum of product of FTR RVs in terms of multivariate Fox's H -function [14, eq. (A-1)], which are given in the following Theorem.

Theorem 3. We define $Y = \sum_{\iota=1}^L X_{\iota}$. Thus, the PDF and CDF of Y can be deduced in closed-form as

$$f_Y(y) = \sum_{j_{1,1}, \dots, j_{L,1}=0}^{\infty} \dots \sum_{j_{1,N}, \dots, j_{L,N}=0}^{\infty} \prod_{\iota=1}^L \prod_{\ell=1}^N \frac{K_{\iota,\ell} j_{\iota,\ell}^{j_{\iota,\ell}} d_{\iota,\ell} j_{\iota,\ell}}{j_{\iota,\ell}!} \frac{m_{\iota,\ell}^{m_{\iota,\ell}}}{\Gamma(m_{\iota,\ell})} \frac{1}{\Gamma(j_{\iota,\ell} + 1)} \frac{1}{y} \\ \times H_{1,0:N,1;\dots;N,1}^{0,0:1,N;\dots;1,N} \left(\begin{array}{c} y^{-1} \prod_{\ell=1}^N (\sqrt{2}\sigma_{1,\ell}) \\ \vdots \\ y^{-1} \prod_{\ell=1}^N (\sqrt{2}\sigma_{L,\ell}) \end{array} \middle| \begin{array}{c} (0; 1, \dots, 1) : \{(-j_{1,n}, 0.5)\}_1^N; \dots; \{(-j_{L,n}, 0.5)\}_1^N \\ - : (0, 1); \dots; (0, 1) \end{array} \right), \quad (11)$$

$$F_Y(y) = \sum_{j_{1,1}, \dots, j_{L,1}=0}^{\infty} \dots \sum_{j_{1,N}, \dots, j_{L,N}=0}^{\infty} \prod_{\iota=1}^L \prod_{\ell=1}^N \frac{K_{\iota,\ell} j_{\iota,\ell}^{j_{\iota,\ell}} d_{\iota,\ell} j_{\iota,\ell}}{j_{\iota,\ell}!} \frac{m_{\iota,\ell}^{m_{\iota,\ell}}}{\Gamma(m_{\iota,\ell})} \frac{1}{\Gamma(j_{\iota,\ell} + 1)} \\ \times H_{1,0:N,1;\dots;N,1}^{0,0:1,N;\dots;1,N} \left(\begin{array}{c} y^{-1} \prod_{\ell=1}^N (\sqrt{2}\sigma_{1,\ell}) \\ \vdots \\ y^{-1} \prod_{\ell=1}^N (\sqrt{2}\sigma_{L,\ell}) \end{array} \middle| \begin{array}{c} (1; 1, \dots, 1) : \{(-j_{1,n}, 0.5)\}_1^N; \dots; \{(-j_{L,n}, 0.5)\}_1^N \\ - : (0, 1); \dots; (0, 1) \end{array} \right) \quad (12)$$

where $\{(a_n)\}_1^N = (a_1), \dots, (a_N)$.

Proof: Please refer to Appendix B. ■

Remark 3. Although the numerical evaluation for multivariate Fox's H -function is unavailable in popular mathematical packages such as MATLAB and Mathematica, its efficient implementations have been reported in recent literature.. For example, a Python implementation for the multivariable Fox's H -function is presented in [19], and an efficient GPU-oriented MATLAB routine for the multivariate Fox's H -function is introduced in [20]. In the following, we will utilize these novel implementations to evaluate our results.

3) *SNR Analysis:* The channel coefficients between the BS and the RIS are denoted by an $L \times 1$ vector \mathbf{h} , where the elements of \mathbf{h} are i.n.i.d. FTR RVs. However, under the FTR model, because the complex baseband voltage of a wireless channel experiencing multipath fading contains two fluctuating specular components with different phases, the elements of \mathbf{h} will have different phases. Besides, the angle of departure (AoD) and angle of arrival (AoA) of a signal will also cause phase difference [21]. Thus, \mathbf{h} can be written as

$$\mathbf{h} = [h_1 e^{i\theta_{1,1}}, \dots, h_L e^{i\theta_{L,1}}]^H \quad (13)$$

where h_ℓ denotes the amplitude of the channel coefficient and $e^{i\theta_{\ell,1}}$ is the corresponding phase. Similarly, the channel coefficients between the RIS and the user can be expressed as an $L \times 1$ vector \mathbf{g} , and the elements are also i.n.i.d. FTR RVs having different phase shifts. The channel coefficient vector \mathbf{g} can be expressed as

$$\mathbf{g} = [g_1 e^{i\theta_{1,2}}, \dots, g_L e^{i\theta_{L,2}}] \quad (14)$$

where g_ℓ represents the amplitude of the channel coefficient and $e^{i\theta_{\ell,2}}$ denotes the corresponding phase. Then, we focus on the downlink of the RIS-aided system. The signal received from the BS through the RIS for the user is given by

$$y = \sqrt{P} \mathbf{g} \Phi \mathbf{h} \mathbf{f}^H s + n \quad (15)$$

where P is the transmit power, $\mathbf{f} \in C^{1 \times L}$ is the beamforming vector satisfying $\|\mathbf{f}\|^2 = 1$, s is transmit signal satisfying $\mathbb{E}[|s|^2] = 1$, $n \sim \mathcal{CN}(0, \sigma^2)$ denotes the additive white Gaussian noise (AWGN) at the user, $\Phi = \beta \text{diag}[e^{i\phi_1}, \dots, e^{i\phi_L}]$, $\beta \in (0, 1]$ is the fixed amplitude reflection coefficient³ and ϕ_1, \dots, ϕ_L are the phase shifts which can be optimized by the RIS controller.

³In practice, each element of the RIS is usually designed to maximize the signal reflection. Thus, we set $\beta = 1$ for simplicity.

Using the maximum ratio transmitting at BS, we can define \mathbf{f} as

$$\mathbf{f} = \frac{\mathbf{g}\Phi\mathbf{h}}{\|\mathbf{g}\Phi\mathbf{h}\|}. \quad (16)$$

Accordingly, the SNR of RIS-aided system is given by

$$\gamma_{\text{RIS}} = \frac{\|\mathbf{g}\Phi\mathbf{h}\|^2 P}{\sigma^2}. \quad (17)$$

Before designing the phase shift, we can theoretically obtain the maximum of γ_{RIS} with the optimal phase shift design of RIS's reflector array as

$$\gamma_{\text{RIS}}^{\max} = \frac{P}{\sigma^2} \left(\sum_{\ell=1}^L h_{\ell} g_{\ell} \right)^2. \quad (18)$$

Corollary 1. *The PDF and CDF of the end-to-end SNR for RIS-aided system, γ_{RIS} , can be derived as*

$$\begin{aligned} f_{\gamma_{\text{RIS}}}(z) = & \frac{1}{2z} \sum_{j_{1,1}, \dots, j_{L,1}=0}^{\infty} \sum_{j_{1,N}, \dots, j_{L,2}=0}^{\infty} \prod_{\iota=1}^L \prod_{\ell=1}^2 \frac{K_{\iota,\ell}^{j_{\iota,\ell}} d_{\iota,\ell} j_{\iota,\ell} m_{\iota,\ell}^{m_{\iota,\ell}}}{j_{\iota,\ell}!} \frac{1}{\Gamma(m_{\iota,\ell}) \Gamma(j_{\iota,\ell} + 1)} \\ & \times H_{1,0:2,1;\dots;2,1}^{0,0:1,2;\dots;1,2} \left(\begin{array}{c} \left(\frac{P}{\sigma^2 z} \right)^{\frac{1}{2}} \prod_{\ell=1}^2 (\sqrt{2}\sigma_{1,\ell}) \\ \vdots \\ \left(\frac{P}{\sigma^2 z} \right)^{\frac{1}{2}} \prod_{\ell=1}^2 (\sqrt{2}\sigma_{L,\ell}) \end{array} \middle| \begin{array}{l} (0; 1, \dots, 1) : \{(-j_{1,n}, 0.5)\}_1^2; \dots; \{(-j_{L,n}, 0.5)\}_1^2 \\ - : (0, 1); \dots; (0, 1) \end{array} \right), \end{aligned} \quad (19)$$

$$\begin{aligned} F_{\gamma_{\text{RIS}}}(z) = & \sum_{j_{1,1}, \dots, j_{L,1}=0}^{\infty} \sum_{j_{1,N}, \dots, j_{L,2}=0}^{\infty} \prod_{\iota=1}^L \prod_{\ell=1}^2 \frac{K_{\iota,\ell}^{j_{\iota,\ell}} d_{\iota,\ell} j_{\iota,\ell} m_{\iota,\ell}^{m_{\iota,\ell}}}{j_{\iota,\ell}!} \frac{1}{\Gamma(m_{\iota,\ell}) \Gamma(j_{\iota,\ell} + 1)} \\ & \times H_{1,0:2,1;\dots;2,1}^{0,0:1,2;\dots;1,2} \left(\begin{array}{c} \left(\frac{P}{\sigma^2 z} \right)^{\frac{1}{2}} \prod_{\ell=1}^2 (\sqrt{2}\sigma_{1,\ell}) \\ \vdots \\ \left(\frac{P}{\sigma^2 z} \right)^{\frac{1}{2}} \prod_{\ell=1}^2 (\sqrt{2}\sigma_{L,\ell}) \end{array} \middle| \begin{array}{l} (1; 1, \dots, 1) : \{(-j_{1,n}, 0.5)\}_1^2; \dots; \{(-j_{L,n}, 0.5)\}_1^2 \\ - : (0, 1); \dots; (0, 1) \end{array} \right). \end{aligned} \quad (20)$$

Proof: Using Theorem 3 and letting $N = 2$, we obtain the PDF and CDF of the sum of product of two FTR RVs. With the help of (18), eqs. (19) and (20) can be derived after some transformation of RVs, which completes the proof. ■

C. Exact Statistics of the End-to-End SNR For AF Relay System

We consider the classic AF relay protocol where the transmission is divided into two equal-sized phases. The transmit power of BS is P_1 in the first phase, and one of AF relay is P_2 in the second phase. Assuming variable gain relays, the end-to-end SNR of AF relay communication system is given as [11]

$$\gamma_{AF} = \frac{\gamma_1 \gamma_2}{d_h \gamma_1 \gamma_2 + c_{h,1} \gamma_1 + c_{h,2} \gamma_2 + 1} \quad (21)$$

where $c_{h,i} = 1 + \kappa_i^2$ and $d_h \triangleq \kappa_1^2 \kappa_2^2 + \kappa_1^2 + \kappa_2^2$. Eq. (21) can be tightly approximated at medium and high SNRs as [22, eq. (9)]

$$\gamma_{AF} \approx \frac{\gamma_1 \gamma_2}{d_h \gamma_1 \gamma_2 + c_{h,1} \gamma_1 + c_{h,2} \gamma_2}. \quad (22)$$

For ideal hardware, i.e. $c_{h,i} = 1$ and $d_h = 0$, Eq. (22) reduces to the half-harmonic mean of γ_ℓ as [23]

$$\gamma_{AF} \approx \frac{\gamma_1 \gamma_2}{\gamma_1 + \gamma_2}. \quad (23)$$

Assuming that $\gamma_i = \frac{P_i}{\sigma^2} |q_i|^2$, ($i = 1, 2$), we can rewrite (22) as

$$\gamma_{AF} \approx \frac{P_1 P_2}{\sigma^2} \frac{|q_1|^2 |q_2|^2}{d |q_1|^2 |q_2|^2 + c_1 |q_1|^2 + c_2 |q_2|^2} = \frac{P_1 P_2}{\sigma^2} Z \quad (24)$$

where $d = P_1 P_2 d_h$ and $c_i = P_i c_{h,i}$, ($i = 1, 2$).

An integral representation for the PDF of γ_{AF} in (22) assuming arbitrarily distributed γ_ℓ and considering hardware impairments is given by

$$f_{\gamma_{AF}}(\gamma) = \frac{c_1 c_2 \gamma}{(1 - \gamma d)^3} \int_0^1 f_{\gamma_1} \left(\frac{c_2 \gamma}{(1 - \gamma d) t} \right) f_{\gamma_2} \left(\frac{c_1 \gamma}{(1 - \gamma d)(1 - t)} \right) \frac{dt}{t^2 (1 - t)^2}. \quad (25)$$

To derive a generic analytical expression for the CDF of the end-to-end SNR of AF relay systems with hardware impairments, we first present the following useful Lemma.

Lemma 1. *An integral representation for the CDF of γ_{AF} in (22) assuming arbitrarily distributed γ and considering hardware impairments is given by*

$$F_{\gamma_{AF}}(\gamma) = 1 - \frac{\gamma c_1}{(1 - \gamma d)} \int_0^1 f_{\gamma_2} \left(\frac{\gamma c_1}{(1 - \gamma d) t} \right) \frac{dt}{t^2} + \frac{\gamma c_1}{(1 - \gamma d)} \times \int_0^1 F_{\gamma_1} \left(\frac{\gamma c_2}{(1 - \gamma d)(1 - t)} \right) f_{\gamma_2} \left(\frac{\gamma c_1}{(1 - \gamma d) t} \right) \frac{dt}{t^2}. \quad (26)$$

Proof: Please refer to Appendix C. ■

For the special case of FTR-distributed hops, closed-form expressions will be derived for both cases of non-ideal and ideal hardware.

Theorem 4. *The PDF and CDF of Z considering hardware impairments and FTR-distributed hops can be deduced in closed-form as*

$$f_Z(z) = \frac{c_2 c_1 z}{(1-zd)^3} \sum_{j_1=0}^{\infty} \sum_{j_2=0}^{\infty} \prod_{\ell=1}^2 \left(\frac{m_\ell^{m_\ell} K_\ell^{j_\ell} d_{\ell j_\ell}}{\Gamma(m_\ell) j_\ell!} \frac{A_\ell^{j_\ell}}{2\sigma_\ell^2 \Gamma(j_\ell + 1)} \right) \\ \times H_{0,1:2,0;2,0}^{0,0:0,2;0,2} \left(\begin{array}{c} A_1^{-1} \\ A_2^{-1} \end{array} \middle| \begin{array}{l} - : (1, 1) (2 + j_1, 1); (1, 1) (2 + j_2, 1) \\ (2 + j_1 + j_2; 1, 1) : - \end{array} \right), \quad (27)$$

$$F_Z(z) = 1 - \frac{m_2 m_2}{\Gamma(m_2)} \sum_{j_2=0}^{\infty} \frac{K_2^{j_2} d_{2j_2}}{j_2!} \frac{1}{\Gamma(j_2 + 1)} \Gamma(1 + j_2, A_2) + H_{AF} \quad (28)$$

where $A_1 = \frac{c_2 z}{2\sigma_1^2(1-zd)}$, $A_2 = \frac{c_1 z}{2\sigma_2^2(1-zd)}$ and

$$H_{AF} = \frac{z c_1}{(1-zd)} \sum_{j_1=0}^{\infty} \sum_{j_2=0}^{\infty} \prod_{\ell=1}^2 \left(\frac{m_\ell^{m_\ell} K_\ell^{j_\ell} d_{\ell j_\ell}}{\Gamma(m_\ell) j_\ell!} \frac{1}{\Gamma(j_\ell + 1)} \right) \frac{(A_2)^{j_2}}{2\sigma_2^2} \\ \times H_{0,1:3,1;2,0}^{0,0:1,2;0,2} \left(\begin{array}{c} A_1^{-1} \\ A_2^{-1} \end{array} \middle| \begin{array}{l} - : (0, 1) (-j_1, 1) (1, 1); (1, 1) (2 + j_2, 1) \\ (1 + j_2; 1, 1) : (0, 1); - \end{array} \right). \quad (29)$$

Proof: Please refer to Appendix D. ■

To compare the AF relay system with the RIS-aided system, we consider the ideal hardware to make a fair comparison.

Corollary 2. *For the special case of ideal hardware, the PDF and CDF of γ_{AF} can be deduced in closed-form as*

$$f_Z(z) = \frac{o^4}{P_1 P_2} z \sum_{j_1=0}^{\infty} \sum_{j_2=0}^{\infty} \prod_{\ell=1}^2 \left(\frac{m_\ell^{m_\ell} K_\ell^{j_\ell} d_{\ell j_\ell}}{2\sigma_\ell^2 \Gamma(j_\ell + 1) \Gamma(m_\ell) j_\ell!} \right) \left(\frac{o^2 z}{2\sigma_1^2 P_1} \right)^{j_1} \left(\frac{o^2 z}{2\sigma_2^2 P_2} \right)^{j_2} \\ \times H_{0,1:2,0;2,0}^{0,0:0,2;0,2} \left(\begin{array}{c} \frac{2\sigma_1^2 P_1}{o^2 z} \\ \frac{2\sigma_2^2 P_2}{o^2 z} \end{array} \middle| \begin{array}{l} - : (1, 1) (2 + j_1, 1); (1, 1) (2 + j_2, 1) \\ (2 + j_1 + j_2; 1, 1) : - \end{array} \right), \quad (30)$$

$$\begin{aligned}
F_Z(z) = & 1 - \frac{m_2^{m_2}}{\Gamma(m_2)} \sum_{j_2=0}^{\infty} \frac{K_2^{j_2} d_{2j_2}}{j_2!} \frac{1}{\Gamma(j_2+1)} \Gamma\left(1+j_2, \frac{o^2 z}{2\sigma_2^2 P_2}\right) \\
& + \sum_{j_1=0}^{\infty} \sum_{j_2=0}^{\infty} \prod_{\ell=1}^2 \left(\frac{m_\ell^{m_\ell} K_\ell^{j_\ell} d_{\ell j_\ell}}{\Gamma(m_\ell)} \frac{1}{j_\ell!} \frac{1}{\Gamma(j_\ell+1)} \right) \left(\frac{o^2 z}{2\sigma_2^2 P_2} \right)^{j_2+1} \\
& \times H_{0,1:3,2;2,0}^{0,0:1,2;0,2} \left(\begin{array}{c} \frac{2\sigma_1^2 P_1}{o^2 z} \\ \frac{2\sigma_2^2 P_2}{o^2 z} \end{array} \middle| \begin{array}{c} - : (0, 1) (-j_1, j_1) (1, 1); (1, 1) (2+j_2, 1) \\ (1+j_2; 1, 1) : (0, 1); - \end{array} \right). \quad (31)
\end{aligned}$$

Proof: Setting $c_1 = P_1$, $c_2 = P_2$ and $d = 0$ in (27) and (28), we can obtain (30) and (31) to complete the proof. \blacksquare

D. Truncation Error

To show the effect of infinite series on the performance of the CDF expression of the sum of product of FTR RVs, truncation error is presented in the following. By truncating (12) with the first M terms, we have

$$\begin{aligned}
\hat{F}_Y(y) = & \sum_{j_{1,1}, \dots, j_{L,1}=0}^M \cdots \sum_{j_{1,N}, \dots, j_{L,N}=0}^M \prod_{\ell=1}^L \prod_{\ell=1}^N \frac{K_{\ell,\ell}^{j_{\ell,\ell}} d_{\ell,j_{\ell,\ell}} m_{\ell,\ell}^{m_{\ell,\ell}}}{j_{\ell,\ell}! \Gamma(m_{\ell,\ell}) \Gamma(j_{\ell,\ell}+1)} \\
& \times H_{1,0:N,1;\dots;N,1}^{0,0:1,N;\dots;1,N} \left(\begin{array}{c} y^{-1} \prod_{\ell=1}^N (\sqrt{2}\sigma_{1,\ell}) \\ \vdots \\ y^{-1} \prod_{\ell=1}^N (\sqrt{2}\sigma_{L,\ell}) \end{array} \middle| \begin{array}{c} (1; 1, \dots, 1) : \{(-j_{1,n}, 0.5)\}_1^N; \dots; \{(-j_{L,n}, 0.5)\}_1^N \\ - : (0, 1); \dots; (0, 1) \end{array} \right). \quad (32)
\end{aligned}$$

The truncation error of the area under the $F_Y(y)$ with respect to the first M terms is given by

$$\varepsilon(N) \triangleq F_Y(\infty) - \hat{F}_Y(\infty). \quad (33)$$

Lemma 2. *By truncating (32) with M terms, the truncation error of (33) is given as*

$$\varepsilon(N) \triangleq 1 - \sum_{j_{1,1}, \dots, j_{L,1}=0}^M \cdots \sum_{j_{1,N}, \dots, j_{L,N}=0}^M \prod_{\ell=1}^L \prod_{\ell=1}^N \frac{K_{\ell,\ell}^{j_{\ell,\ell}} d_{\ell,j_{\ell,\ell}} m_{\ell,\ell}^{m_{\ell,\ell}}}{j_{\ell,\ell}! \Gamma(m_{\ell,\ell})}. \quad (34)$$

It can be shown that $\varepsilon(\infty) \rightarrow 0$ as $M \rightarrow \infty$.

Proof: The asymptotic expansions of the multivariate Fox's H -function in (32) can be obtained by

TABLE I
MINIMUM REQUIRED TERMS AND TRUNCATION ERROR FOR DIFFERENT PARAMETERS $m_\ell = m$, $K_\ell = K$, $\Delta_\ell = \Delta$, $\sigma_\ell^2 = \sigma^2$ AND L
WITH $N = 2$

Parameter	$\varepsilon(L)$	L
$L = 1, m = 5, K = 3, \Delta = 0.5, \sigma^2 = 0.5$	6.52×10^{-6}	24
$L = 2, m = 5, K = 3, \Delta = 0.5, \sigma^2 = 0.5$	7.93×10^{-6}	25
$L = 2, m = 25, K = 3, \Delta = 0.5, \sigma^2 = 0.5$	8.51×10^{-6}	17
$L = 3, m = 5, K = 3, \Delta = 0.25, \sigma^2 = 0.5$	8.34×10^{-6}	21

computing the residue [19]. Thus, while $y \rightarrow \infty$, Eq. (32) can be expressed as

$$\hat{F}_Y(y) = \sum_{j_{1,1}, \dots, j_{L,1}=0}^M \cdots \sum_{j_{1,N}, \dots, j_{L,N}=0}^M \prod_{\ell=1}^L \prod_{\ell=1}^N \frac{K_{\ell,\ell}^{j_{\ell,\ell}} d_{\ell,\ell}^{j_{\ell,\ell}} m_{\ell,\ell}^{m_{\ell,\ell}}}{j_{\ell,\ell}! \Gamma(m_{\ell,\ell})}. \quad (35)$$

Furthermore, we have

$$\sum_{j_{1,1}, \dots, j_{L,1}=0}^{\infty} \cdots \sum_{j_{1,N}, \dots, j_{L,N}=0}^{\infty} \prod_{\ell=1}^L \prod_{\ell=1}^N \frac{K_{\ell,\ell}^{j_{\ell,\ell}} d_{\ell,\ell}^{j_{\ell,\ell}} m_{\ell,\ell}^{m_{\ell,\ell}}}{j_{\ell,\ell}! \Gamma(m_{\ell,\ell})} = 1. \quad (36)$$

Then, we complete the proof by using the above result. ■

To demonstrate the convergence of the series in (34), Table I depicts the required truncation terms M for different system and channel parameters. With a satisfactory accuracy (e.g., smaller than 10^{-5}), only less than 30 terms are needed for all considered cases. We also note that the number of truncation terms M slightly increases with the number of RVs L .

III. PHASE SHIFT AND POWER OPTIMIZATION

In this section, we propose an optimal design of Φ to maximize the SNR by exploiting the statistical CSI of the RIS-aided system. We also present an optimal power allocation scheme for the AF relay system.

A. Optimal Phase Shift Design of RIS's Reflector Array

To characterize the fundamental performance limit of RIS, we assume that the phase shifts can be continuously varied in $(0, 2\pi]$, while in practice they are usually selected from a finite number of discrete values to simplify the circuit implementation [24].

Based on (17), maximizing the SNR γ_{RIS} is equivalent to maximizing $\|\mathbf{g}\Phi\mathbf{h}\|^2$. Using (13) and (14), we can rewrite $\|\mathbf{g}\Phi\mathbf{h}\|^2$ as

$$\|\mathbf{g}\Phi\mathbf{h}\|^2 = \left(\sum_{\ell=1}^L h_\ell g_\ell e^{i(\theta_{\ell,1} + \theta_{\ell,2} + \phi_\ell)} \right)^2 \quad (37)$$

where ϕ_ℓ is the adjustable phase induced by the i_{th} reflecting element of the RIS. The optimal choice of ϕ_ℓ can maximizes the instantaneous SNR. Thus, the optimal $\Phi_{\text{opt}s}$ satisfies

$$\Phi_{\text{opt}} = \max_{\phi_\ell} \left| \sum_{\ell=1}^L h_\ell g_\ell e^{i(\theta_{\ell,1} + \theta_{\ell,2} + \phi_\ell)} \right| = \sum_{\ell=1}^L h_\ell g_\ell \max_{\phi_\ell} \left| \sum_{\ell=1}^L e^{i(\theta_{\ell,1} + \theta_{\ell,2} + \phi_\ell)} \right|. \quad (38)$$

According to [25, eq. (12)], it is easy to infer that γ_{RIS} is maximized by eliminating the channel phases (similar to co-phasing in classical maximum ratio combining schemes), i.e., the optimal choice of ϕ_ℓ that maximizes the instantaneous SNR is $\theta_{\ell,1} + \theta_{\ell,2} + \phi_\ell = \phi$ for all i .

However, this solution, notably, requires that the channel phases are perfectly known at the RIS. How to perform channel estimation in RIS-aided system is challenging, because the RIS is assumed to be passive, as opposed to, e.g., the AF relay. Moreover, in [21], the BS is assumed to be equipped with a large uniform linear array; therefore, the problem is transferred to measure the AoD and AoA at the RIS. However, the authors in [21] did not obtain a feasible solution to this problem. Herein, we propose a novel and simple algorithm based on the binary search tree [26]. Note that the maximum achievable expectation of the amplitude of the received signal can be expressed as

$$\mathbb{E} \left[\left| \sum_{\ell=1}^L h_\ell g_\ell e^{i(\theta_{\ell,1} + \theta_{\ell,2} + \phi_\ell)} \right| \right] \leq \mathbb{E} \left[\sum_{\ell=1}^L h_\ell g_\ell \right] = \sum_{\ell=1}^L \mathbb{E}[h_\ell g_\ell] \quad (39)$$

where $\mathbb{E}[h_\ell g_\ell]$ can be calculated with the aid of (6).

Let $E_{\text{re}} \triangleq \mathbb{E} \left[\left| \sum_{\ell=1}^L h_\ell g_\ell e^{i(\theta_{\ell,1} + \theta_{\ell,2} + \phi_\ell)} \right| \right]$ and $E_{\text{opt}} \triangleq \sum_{\ell=1}^L E_\ell = \sum_{\ell=1}^L \mathbb{E}[h_\ell g_\ell]$, and we notice that E_{re} can be easily measured in the time domain and E_{opt} can be calculated directly using the CSI. Thus, when initially setting up the RIS, using the ideal E_{opt} and E_{re} sent from the user, we use the binary search tree algorithm to adjust the reflection angle of the elements on the RIS one by one. For each element, we perform M_1 times of search. After searching all elements, we repeat the same operation M_2 times. The entire algorithm flow is shown in Fig. 3. This solution does not compromise on the almost passive nature of the RIS.

Combining the above discussion, we present our method to find Φ_{opt} as Algorithm 1, where $\text{Mod}[a, b]$ denotes the remainder on division of a by b . Thus, with the optimal phase shift design of RIS's reflector array, we can obtain the maximum of γ_{RIS} as (18).

To investigate the convergence of the proposed phase optimization method, we define the error of expectation as $\zeta \triangleq E_{\text{opt}} - E_{\text{re}}$ and use the variance of $\theta_{\ell,1} + \theta_{\ell,2} + \phi_\ell$ ($\ell = 1, \dots, L$) to characterize the phase error.

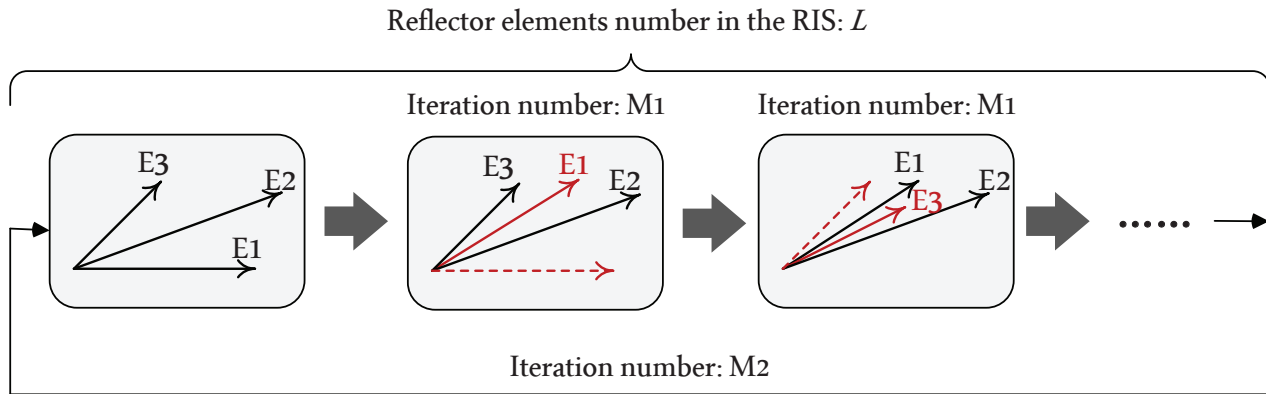


Fig. 3. The binary search tree algorithm for RIS-aided system.

Algorithm 1 The binary search tree algorithm for finding Φ_{opt} .

Input: input the number of elements on RIS: L , the maximum achievable expectation: E_{opt} and E_ℓ ($\ell = 1, \dots, L$), iteration numbers: M_1 and M_2

Output: The phase-shift variable ϕ_ℓ ($\ell = 1, \dots, L$) for each RIS element should be set.

- 1: Initialize $\phi_{\text{LB}} = 0$, $\phi_{\text{UB}} = \pi$ and $\ell_{\text{th}} = 1$. Set iteration index $\text{LP}_1 = \text{LP}_2 = t = 0$.
 - 2: **while** $\text{LP}_2 < M_2$ **do**
 - 3: **while** $\ell_{\text{th}} \leq L$ **do**
 - 4: **while** $\text{LP}_1 < M_1$ **do**
 - 5: When the phase-shift variable of the ℓ_{th} elements is set as ϕ_{LB} and ϕ_{UB} , we use E_{m_1} and E_{m_2} to denote the expectation of the amplitude of the received signal measured at the user, respectively.
 - 6: $t \leftarrow t + 1$
 - 7: **if** $E_{m_1} > E_{m_2}$ **then**
 - 8: $\phi_{\text{LB}} \leftarrow \text{Mod} \left[\phi_{\text{LB}} + \frac{\pi}{2^{t+1}} + 1, 2\pi \right]$ and $\phi_{\text{UB}} \leftarrow \text{Mod} \left[\phi_{\text{LB}} - \frac{\pi}{2^t}, 2\pi \right]$.
 - 9: **else**
 - 10: $\phi_{\text{UB}} \leftarrow \text{Mod} \left[\phi_{\text{UB}} + \frac{\pi}{2^{t+1}}, 2\pi \right]$ and $\phi_{\text{LB}} \leftarrow \text{Mod} \left[\phi_{\text{UB}} - \frac{\pi}{2^t}, 2\pi \right]$.
 - 11: $\text{LP}_1 \leftarrow \text{LP}_1 + 1$
 - 12: $\ell_{\text{th}} \leftarrow \ell_{\text{th}} + 1$, $t \leftarrow 0$ and $\text{LP}_1 \leftarrow 0$.
 - 13: $\text{LP}_2 \leftarrow \text{LP}_2 + 1$, $\phi_\ell \leftarrow \text{Mod} [\phi_\ell + \phi_{\text{LB}}]$, $\phi_{\text{LB}} \leftarrow 0$ and $\phi_{\text{UB}} \leftarrow 0$
 - 14: **return** ϕ_ℓ ($\ell = 1, \dots, L$)
-

In Figs. 4 and 5, we verify the effectiveness of the proposed algorithm for different iteration numbers M_1 and M_2 . Figures 4 and 5, respectively, plot an example of the expectation and phase error, assuming $L = 3$, $\theta_{1,1} + \theta_{1,2} = \pi/4$, $\theta_{2,1} + \theta_{2,2} = \pi/2$, $\theta_{3,1} + \theta_{3,2} = \pi/8$, $m_{1,1} = m_{1,2} = 10$, $K_{1,1} = K_{1,2} = 3$, $v_{1,1} = v_{1,2} = 10$, $\delta_{1,1} = \delta_{1,2} = 0.5$, $m_{2,1} = m_{2,2} = 5$, $K_{2,1} = K_{2,2} = 5$, $v_{2,1} = v_{2,2} = 20$, $\delta_{2,1} = \delta_{2,2} = 0.5$, $m_{3,1} = m_{3,2} = 15$, $K_{3,1} = K_{3,2} = 1$, $v_{3,1} = v_{3,2} = 10$ and $\delta_{3,1} = \delta_{3,2} = 0.3$. Using (6), we obtain $E_1 = 8.36$, $E_2 = 12.79$, $E_3 = 8.16$ and $E_{\text{opt}} = 29.33$. Thus, substituting E_1 , E_2 , E_3 and E_{opt} into Algorithm 1, we obtain $\phi_1 = 0.076$, $\phi_2 = 5.575$, $\phi_3 = 0.469$ and $\phi = 0.86$. To obtain a satisfactory accuracy (e.g., smaller than 10^{-6}), only less than 50 iteration numbers are needed for each element.

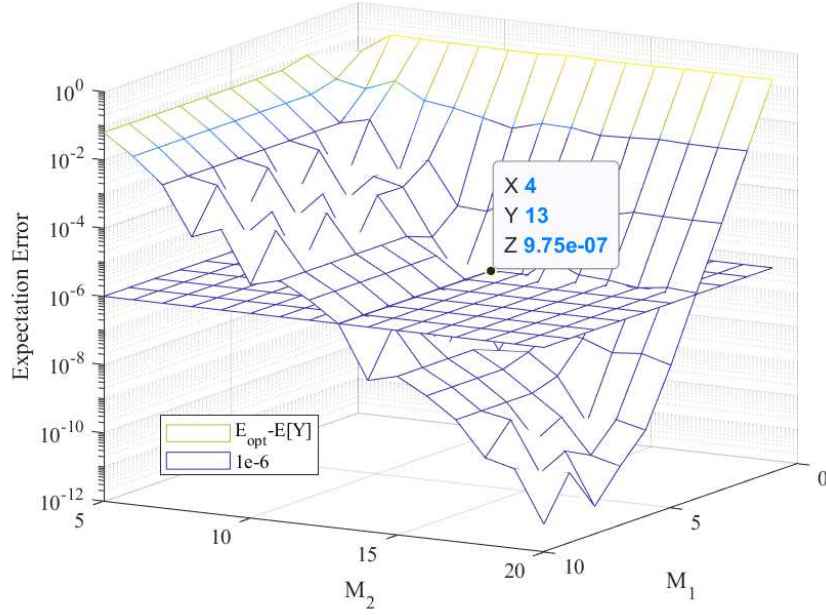


Fig. 4. The expectation error of the proposed phase optimization method.

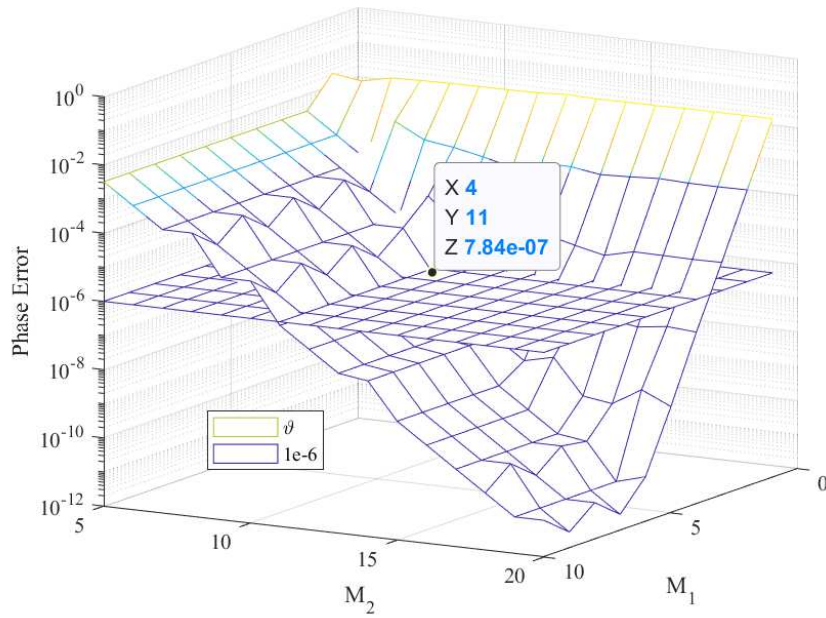


Fig. 5. The phase error of the proposed phase optimization method.

B. Optimal power allocation scheme for the AF relay system

To make a fair comparison, we first select P_1 and P_2 optimally, while having the same average power P as when using the RIS. Assuming that P_1 and P_2 are selected under the constraint $P_1 + P_2 = 2P$ and

using (24), we can obtain

$$\frac{1}{o^2\gamma_{AF}} = \left(\frac{1}{|q_2|^2 P_2} + \frac{1}{|q_1|^2 (2P - P_2)} \right). \quad (40)$$

Thus, we derive the derivative of $\frac{1}{o^2\gamma_{AF}}$ as

$$\left(\frac{1}{o^2\gamma_{AF}} \right)' = \frac{1}{|q_1|^2 (2P - P_2)^2} - \frac{1}{|q_2|^2 P_2^2}. \quad (41)$$

With the help of (41)

$$P_1 = \frac{2P|q_2|}{|q_1| + |q_2|}, P_2 = \frac{2P|q_1|}{|q_1| + |q_2|}. \quad (42)$$

Substituting (42) into (24), we obtain the maximum of γ_{AF} as

$$\gamma_{AF}^{\max} = \frac{2P}{o^2} \frac{|q_1|^2 |q_2|^2}{(|q_1| + |q_2|)^2}. \quad (43)$$

Corollary 3. *The PDF and CDF expressions of γ_{AF}^{\max} can be derived as*

$$\begin{aligned} f_{\gamma_{AF}^{\max}}(z) &= \frac{o^2}{P} \sum_{j_1=0}^{\infty} \sum_{j_2=0}^{\infty} \prod_{\ell=1}^2 \left(\frac{m_{\ell}^{m_{\ell}} K_{\ell}^{j_{\ell}} d_{\ell j_{\ell}}}{\Gamma(m_{\ell}) j_{\ell}!} \frac{\left(\frac{o^2}{2P} z\right)^{1+j_1+j_2}}{(2\sigma_{\ell}^2)^{j_{\ell}+1} \Gamma(j_{\ell}+1)} \right) \\ &\times H_{0,1:2,0;2,0}^{0,0:0,2;0,2} \left(\begin{array}{c} \frac{4P\sigma_1^2}{o^2 z} \\ \frac{4P\sigma_2^2}{o^2 z} \end{array} \middle| \begin{array}{c} - : (2, 2) (3 + 2j_1, 2); (2, 2) (3 + 2j_2, 2) \\ (4 + 2j_1 + 2j_2; 2, 2) : - \end{array} \right), \end{aligned} \quad (44)$$

$$\begin{aligned} F_{\gamma_{AF}^{\max}}(z) &= 1 - \frac{m_2^{m_2}}{\Gamma(m_2)} \sum_{j_2=0}^{\infty} \frac{K_2^{j_2} d_{2j_2}}{j_2!} \frac{1}{\Gamma(j_2+1)} \Gamma\left(1 + j_2, \frac{o^2 z}{4P\sigma_2^2}\right) \\ &+ 2 \sum_{j_1=0}^{\infty} \sum_{j_2=0}^{\infty} \prod_{\ell=1}^2 \left(\frac{m_{\ell}^{m_{\ell}} K_{\ell}^{j_{\ell}} d_{\ell j_{\ell}}}{\Gamma(m_{\ell}) j_{\ell}!} \frac{1}{\Gamma(j_{\ell}+1)} \right) \frac{(o^2 z)^{1+j_2}}{(4P\sigma_2^2)^{j_2+1}} \\ &\times H_{0,1:3,1;2,0}^{0,0:1,2;0,2} \left(\begin{array}{c} \frac{4P\sigma_1^2}{o^2 z} \\ \frac{4P\sigma_2^2}{o^2 z} \end{array} \middle| \begin{array}{c} - : (0, 2) (-j_1, 1) (1, 1); (1, 1) (3 + 2j_2, 2) \\ (1 + 2j_2; 2, 2) : (0, 1); - \end{array} \right). \end{aligned} \quad (45)$$

Proof: Substituting $R = \sqrt{\gamma}$ into (1) and (2), the PDF and CDF of $\frac{|q_1||q_2|}{|q_1|+|q_2|}$ can be derived easily following the similar procedures as in Theorem 4. Employing a transformation of RVs, the CDF of γ_{AF}^{\max} can be derived to complete the proof. ■

IV. PERFORMANCE ANALYSIS OF TWO SYSTEMS

In this section, we compare the performance of the RIS-aided and AF relay systems in terms of OP and ABEP, respectively.

A. Outage Probability

The outage probability P is defined as the probability that the received SNR per signal falls below a given threshold γ_{th} . Thus, the OP can be obtained as

$$P_{out} = P(\gamma < \gamma_{th}) = F_{\gamma}(\gamma_{th}). \quad (46)$$

Therefore, the OP of the RIS-aided and AF relay system can be directly evaluated by using (20) and (31), respectively.

B. Average Bit Error Probability

Another important performance metric frequently applied is the ABEP, which is given by [12]

$$P_e = \frac{q^p}{2\Gamma(p)} \int_0^{\infty} z^{p-1} e^{-qz} F_Z(z) dz \quad (47)$$

where p and q denote the modulation-specific parameters for binary modulation schemes, respectively. For instance, $(p, q) = (0.5, 1)$ denotes the binary shift keying (BPSK), $(p, q) = (0.5, 0.5)$ for coherent binary frequency shift keying, and $(p, q) = (1, 1)$ for differential BPSK [27].

Proposition 1. *The exact ABEP of RIS-aided system can be expressed as*

$$P_e = \frac{1}{2\Gamma(p)} \sum_{j_{1,1}, \dots, j_{L,1}=0}^{\infty} \sum_{j_{1,2}, \dots, j_{L,2}=0}^{\infty} \prod_{\iota=1}^L \prod_{\ell=1}^2 \frac{K_{\iota,\ell}^{j_{\iota,\ell}} d_{\iota,\ell}^{j_{\iota,\ell}} m_{\iota,\ell}^{m_{\iota,\ell}}}{j_{\iota,\ell}!} \frac{1}{\Gamma(m_{\iota,\ell}) \Gamma(j_{\iota,\ell} + 1)} H_{BEP}^{LIS} \quad (48)$$

where

$$H_{BEP}^{LIS} = H_{2,0:1,1;\dots;1,1}^{0,1:1,1;\dots;1,1} \left(\begin{matrix} \left(\frac{qP}{\sigma^2} \right)^{\frac{1}{2}} \prod_{\ell=1}^2 (\sqrt{2}\sigma_{1,\ell}) \\ \vdots \\ \left(\frac{qP}{\sigma^2} \right)^{\frac{1}{2}} \prod_{\ell=1}^2 (\sqrt{2}\sigma_{L,\ell}) \end{matrix} \middle| \begin{matrix} (1-p; -0.5, \dots, -0.5) (1; 1, \dots, 1) : \eta \\ - : (0, 1); \dots; (0, 1) \end{matrix} \right), \quad (49)$$

and

$$\eta = \{(-j_{1,n}, 0.5)\}_1^2; \dots; \{(-j_{L,n}, 0.5)\}_1^2. \quad (50)$$

Proof: Substituting (12) in (47) and changing the order of integration, we can obtain

$$P_e = \sum_{j_{1,1}, \dots, j_{L,1}=0}^{\infty} \cdots \sum_{j_{1,N}, \dots, j_{L,N}=0}^{\infty} \prod_{\ell=1}^L \prod_{\ell=1}^N \frac{K_{\ell, \ell}^{j_{\ell, \ell}} d_{\ell, \ell}^{j_{\ell, \ell}} m_{\ell, \ell}^{m_{\ell, \ell}}}{j_{\ell, \ell}! \Gamma(m_{\ell, \ell}) \Gamma(j_{\ell, \ell} + 1)} \frac{1}{\Gamma(j_{\ell, \ell} + 1)} \\ \times \prod_{\iota=1}^L \frac{1}{2\pi i} \int_{\mathcal{L}_\iota} \frac{\prod_{\ell=1}^N \Gamma(1 + j_{\ell, \ell} + \frac{1}{2} s_\ell) \Gamma(-s_\ell)}{\Gamma(1 - \sum_{\ell=1}^L s_\ell)} \left(\left(\frac{P}{o^2} \right)^{\frac{1}{2}} \prod_{\ell=1}^N (\sqrt{2} \sigma_{\ell, \ell}) \right)^{s_\ell} d s_\ell \frac{q^p}{2\Gamma(p)} I_{D_1} \quad (51)$$

where

$$I_{D_1} = \int_0^\infty z^{-0.5 \sum_{\iota=1}^N s_\iota + p - 1} e^{-qz} dz. \quad (52)$$

With the help of [13, eq. (3.351.3)] and [13, eq. (8.331.1)], I_{D_1} can be expressed as

$$I_{D_1} = q^{-p + 0.5 \sum_{\iota=1}^N s_\iota} \Gamma \left(p - 0.5 \sum_{\iota=1}^N s_\iota \right). \quad (53)$$

Letting $N = 2$ and substituting (53) in (51), we obtain

$$P_e = \frac{1}{2\Gamma(p)} \sum_{j_{1,1}, \dots, j_{L,1}=0}^{\infty} \cdots \sum_{j_{1,N}, \dots, j_{L,N}=0}^{\infty} \prod_{\ell=1}^L \prod_{\ell=1}^N \frac{K_{\ell, \ell}^{j_{\ell, \ell}} d_{\ell, \ell}^{j_{\ell, \ell}} m_{\ell, \ell}^{m_{\ell, \ell}}}{j_{\ell, \ell}! \Gamma(m_{\ell, \ell}) \Gamma(j_{\ell, \ell} + 1)} \frac{1}{\Gamma(j_{\ell, \ell} + 1)} \\ \times \prod_{\iota=1}^L \frac{1}{2\pi i} \int_{\mathcal{L}_\iota} \prod_{\ell=1}^2 \Gamma \left(1 + j_{\ell, \ell} + \frac{1}{2} s_\ell \right) \Gamma(-s_\ell) \frac{\Gamma \left(p - 0.5 \sum_{\iota=1}^N s_\iota \right)}{\Gamma \left(1 - \sum_{\iota=1}^L s_\iota \right)} \left(\left(\frac{qP}{o^2} \right)^{\frac{1}{2}} \prod_{\ell=1}^2 (\sqrt{2} \sigma_{\ell, \ell}) \right)^{s_\ell} d s_\iota. \quad (54)$$

With the help of [14, eq. (A-1)], eq. (54) can be expressed as (48) which completes the proof. \blacksquare

Proposition 2. *The exact ABEP of AF relay system with any P_1 and P_2 can be expressed as*

$$P_e^{AF} = \frac{1}{2} - \frac{m_2^{m_2}}{2\Gamma(p)\Gamma(m_2)} \sum_{j_2=0}^{\infty} \frac{K_2^{j_2} d_2^{j_2} \Gamma(p+1+j_2)}{j_2! \Gamma(j_2+1)} \frac{{}_2F_1 \left(1, p+1+j_2; p+1; \frac{2\sigma_2^2 P_2 q}{o^2 + 2\sigma_2^2 P_2 q} \right)}{\left(\frac{o^2}{2P_2 \sigma_2^2 q} + 1 \right)^{-p} p \left(1 + \frac{2P_2 \sigma_2^2 q}{o^2} \right)^{1+j_2}} \\ + \frac{q^{-1-j_2}}{2\Gamma(p)} \sum_{j_1=0}^{\infty} \sum_{j_2=0}^{\infty} \prod_{\ell=1}^2 \left(\frac{m_\ell^{m_\ell} K_\ell^{j_\ell} d_\ell^{j_\ell}}{\Gamma(m_\ell) j_\ell! \Gamma(j_\ell+1)} \frac{1}{\Gamma(j_\ell+1)} \right) \left(\frac{o^2}{2\sigma_2^2 P_2} \right)^{j_2+1} \\ \times H_{1,1:3,1;2,0}^{0,1:1,2;0,2} \left(\begin{array}{c} \frac{2\sigma_1^2 P_1 q}{o^2} \\ \frac{2\sigma_2^2 P_2 q}{o^2} \end{array} \middle| \begin{array}{c} (-j_2 - p, -1, -1) : (-j_1, 1) (0, 1) (0, 1); (2 + j_2, 1) (1, 1) \\ (1 + j_2, 1, 1) : (1, 1); - \end{array} \right). \quad (55)$$

Proof: Substituting (31) into (47), we obtain

$$\begin{aligned}
P_e^{AF} &= \frac{q^p}{2\Gamma(p)} I_{E_1} - \frac{q^p}{2\Gamma(p)} \frac{m_2^{m_2}}{\Gamma(m_2)} \sum_{j_2=0}^{\infty} \frac{K_2^{j_2} d_{2j_2}}{j_2!} \frac{1}{\Gamma(j_2+1)} I_{E_2} \\
&+ \frac{q^p}{2\Gamma(p)} \sum_{j_1=0}^{\infty} \sum_{j_2=0}^{\infty} \prod_{\ell=1}^2 \left(\frac{m_\ell^{m_\ell} K_\ell^{j_\ell} d_{\ell j_\ell}}{\Gamma(m_\ell)} \frac{1}{j_\ell!} \frac{1}{\Gamma(j_\ell+1)} \right) \left(\frac{1}{2\sigma_2^2} \right)^{j_2+1} \left(\frac{1}{2\pi i} \right)^2 \int_{\mathcal{L}_1} \int_{\mathcal{L}_2} I_{E_3} \\
&\times \frac{\Gamma(s_1+j_1+1) \Gamma(1+s_1) \Gamma(-s_1) \Gamma(s_2) \Gamma(s_2-j_2-1)}{\Gamma(1-s_1) \Gamma(s_1+s_2-j_2)} \left(\frac{o^2}{2P_2\sigma_2^2} \right)^{-s_2} \left(\frac{o^2}{2P_1\sigma_1^2} \right)^{-s_1} ds_2 ds_1
\end{aligned} \tag{56}$$

where

$$I_{E_1} = \int_0^\infty z^{p-1} e^{-qz} dz, \tag{57}$$

$$I_{E_2} = \int_0^\infty z^{p-1} e^{-qz} \Gamma\left(1+j_2, \frac{o^2 z}{2P_2\sigma_2^2}\right) dz, \tag{58}$$

and

$$I_{E_3} = \int_0^\infty z^{p-s_1-s_2+j_2} e^{-qz} dz. \tag{59}$$

Following similar procedures as (52), using [13, eq. (3.351.3)] and [13, eq. (8.331.1)], we can solve I_{E_1} and I_{E_3} respectively as

$$I_{E_1} = q^{-p} \Gamma(p) \tag{60}$$

and

$$I_{E_3} = q^{-1-j_2-p+s_1+s_2} \Gamma(1+j_2+p-s_1-s_2). \tag{61}$$

With the help of [13, eq. (6.455.1)], I_{E_2} can be solved as

$$I_{E_2} = \frac{\Gamma(p+1+j_2) \left(\frac{2P_2\sigma_2^2}{o^2}\right)^p}{p\left(1+\frac{2P_2\sigma_2^2}{o^2}q\right)^{p+1+j_2}} {}_2F_1\left(1, p+1+j_2; p+1; \frac{q}{\frac{1}{2\sigma_2^2}+q}\right). \tag{62}$$

Substituting (60), (62) and (61) into (56), we derive (55) to complete the proof. ■

Proposition 3. *The exact ABEP of AF relay system with optimally selected P_1 and P_2 can be expressed*

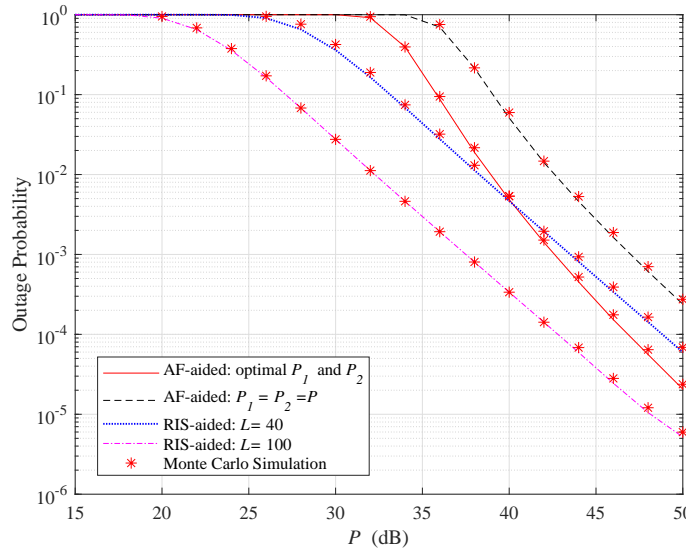


Fig. 6. Outage probability of the RIS-aided and AF relay systems versus the transmit power with $\sigma_N = 0$ dB, $r_{th} = 1$, $m_{\ell,1} = 5$, $m_{\ell,2} = 10$, $K_{\ell,1} = 5$, $K_{\ell,2} = 7$, $\delta_{\ell,1} = 0.5$, $\delta_{\ell,2} = 0.7$, $v = -60$ dB.

as

$$\begin{aligned}
P_e^{AF} = & \frac{1}{2} - \frac{m_2^{m_2}}{2\Gamma(p)\Gamma(m_2)} \sum_{j_2=0}^{\infty} \frac{K_2^{j_2} d_2^{j_2} \Gamma(p+1+j_2)}{j_2! \Gamma(j_2+1)} \frac{{}_2F_1\left(1, p+1+j_2; p+1; \frac{4\sigma_2^2 P q}{o^2+4\sigma_2^2 P q}\right)}{\left(\frac{o^2}{4P\sigma_2^2 q} + 1\right)^{-p} p \left(1 + \frac{4P\sigma_2^2 q}{o^2}\right)^{1+j_2}} \\
& + \frac{q^{-1-j_2}}{\Gamma(p)} \sum_{j_1=0}^{\infty} \sum_{j_2=0}^{\infty} \prod_{\ell=1}^2 \left(\frac{m_{\ell}^{m_{\ell}} K_{\ell}^{j_{\ell}} d_{\ell}^{j_{\ell}}}{\Gamma(m_{\ell}) j_{\ell}! \Gamma(j_{\ell}+1)} \frac{1}{\Gamma(j_{\ell}+1)} \right) \left(\frac{o^2}{4P\sigma_2^2} \right)^{j_2+1} \\
& \times H_{1,1:3,1;2,0}^{0,1:1,2;0,2} \left(\begin{array}{c} \frac{4\sigma_1^2 P q}{o^2} \\ \frac{4\sigma_2^2 P q}{o^2} \end{array} \middle| \begin{array}{c} (-j_2 - p; -1, -1) : (-j_1, 1) (0, 1) (0, 1); (2 + j_2, 1) (1, 1) \\ (1 + j_2; 1, 1) : (1, 1); - \end{array} \right). \quad (63)
\end{aligned}$$

Proof: Following similar steps as in Proposition 2, we can easily obtain (63) and complete the proof. ■

V. NUMERICAL RESULTS AND DISCUSSIONS

In this section, numerical results are presented to compare the performance of both RIS-aided and AF relay systems.

Figure 6 depicts the OP performance of the RIS-aided and the AF relay system versus the transmit power with $\sigma_N = 0$, dB, $r_{th} = 1$, $m_{\ell,1} = 5$, $m_{\ell,2} = 10$, $K_{\ell,1} = 5$, $K_{\ell,2} = 7$, $\delta_{\ell,1} = 0.5$, $\delta_{\ell,2} = 0.7$, $v = -60$ dB. As it can be observed, for the RIS-aided system, the OP decreases as the transmit power and L increase. In addition, using the optimal power allocation scheme, we can see that the AF relay system has lower OP than the RIS-aided system with 40 reflecting elements and $P_{um} > 40$ dB, and decays faster

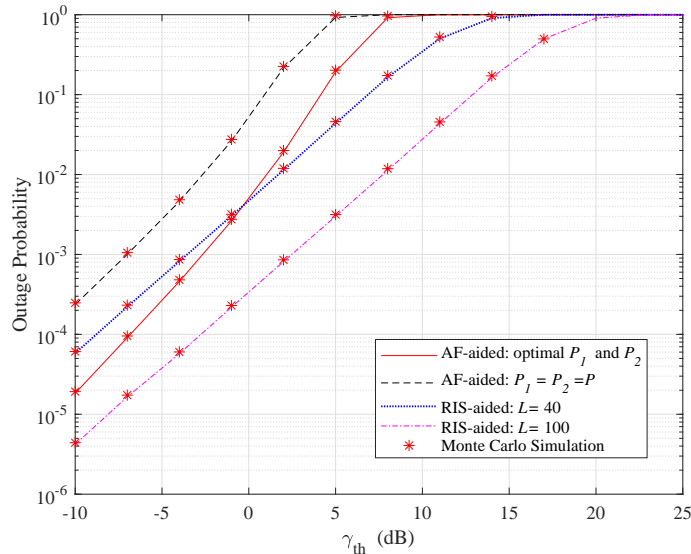


Fig. 7. Outage probability of the RIS-aided and AF relay systems versus the threshold SNR with $\sigma_N = 0$, $P_{um} = 20$ dB, $m_{\ell,1} = 5$, $m_{\ell,2} = 10$, $K_{\ell,1} = 5$, $K_{\ell,2} = 7$, $\delta_{\ell,1} = 0.5$, $\delta_{\ell,2} = 0.7$, $v = -20$ dB..

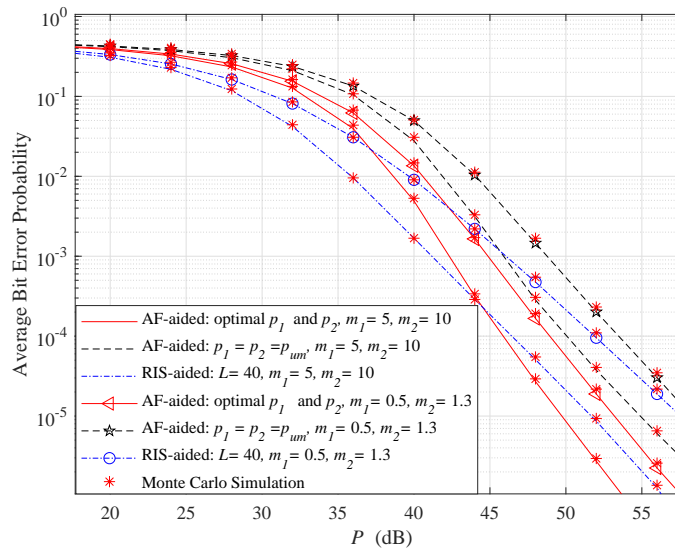


Fig. 8. Average Bit Error Probability of the RIS-aided and AF relay systems versus the transmit power with $\sigma_N = 0$, $v = -60$ dB, $K_{\ell,1} = 5$, $K_{\ell,2} = 7$, $\delta_{\ell,1} = 0.5$, $\delta_{\ell,2} = 0.7$ and different $m_{\ell,1}$ and $m_{\ell,2}$.

than RIS-aided system. If the RIS is equipped with 100 elements, the OP of RIS-aided system is always lower than the AF relay system. Considering that the RIS is usually equipped with hundreds of elements, it is of practical interest to employ RIS in mmWave communications. Furthermore, it is easy to observe from the figure that a good agreement exists between the analytical and simulation results, which justifies the correctness of proposed analytical expressions.

Figure 7 illustrates the OP of the two considered system versus the threshold γ_{th} with $\sigma_N = 0$, $P_{um} = 20$

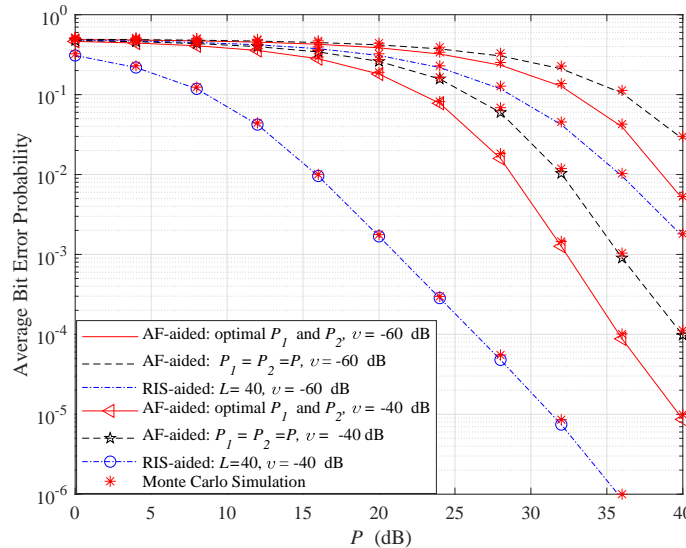


Fig. 9. Average Bit Error Probability of the RIS-aided and AF relay systems versus the transmit power with $\sigma_N = 0$, $m_{\ell,1} = 5$, $m_{\ell,2} = 10$, $K_{\ell,1} = 5$, $K_{\ell,2} = 7$, $\delta_{\ell,1} = 0.5$ and $\delta_{\ell,1} = 0.7$.

dB, $m_{\ell,1} = 5$, $m_{\ell,2} = 10$, $K_{\ell,1} = 5$, $K_{\ell,2} = 7$, $\delta_{\ell,1} = 0.5$, $\delta_{\ell,1} = 0.7$, $v = -20$ dB. An interesting insight is that the OP of AF relay system increases faster than the one of the RIS-aided system. This implies that the RIS can better adapt to the wireless requirements than the AF relay. Again, under the set of channel parameters, the RIS equipped with 100 reflecting elements can achieve a lower OP than the AF relay. The reason is that RIS has superior capability in manipulating electromagnetic waves, thus it can provide space-intensive and reliable communication, enabling the desired wireless channel to exhibit a perfect line-of-sight.

Figure 8 plots the ABEP of the RIS-aided and AF relay systems versus the transmit power with $\sigma_N = 0$, $v = -60$ dB, $K_{\ell,1} = 5$, $K_{\ell,2} = 7$, $\delta_{\ell,1} = 0.5$, $\delta_{\ell,1} = 0.7$ and different $m_{\ell,1}$ and $m_{\ell,2}$. Obviously, the ABEP decreases as the increase of transmit power for both systems. Similar to the OP, the ABEP of AF relay system decreases faster than the one of the RIS-aided system. Moreover, the curves show the impact of different values of shaping parameter $m_{\ell,1}$ and $m_{\ell,2}$. As $m_{\ell,2}$ is decreased, the ABEP decreases because of the worse channel conditions.

As shown in Fig. 9, with $\sigma_N = 0$, $m_{\ell,1} = 5$, $m_{\ell,2} = 10$, $K_{\ell,1} = 5$, $K_{\ell,2} = 7$, $\delta_{\ell,1} = 0.5$ and $\delta_{\ell,1} = 0.7$, the received SNR undergoing the FTR fading channel, v , has a great impact on the performance of the RIS-aided system. We can observe that the ABEP of the RIS-aided system decreases faster than the AF relay system versus the increase of v . It is important to find that, as the channel conditions improve, the performance of the RIS-aided system can outperform the AF relay system with the same transmit power.

The RIS equipped with only 40 elements can also provide a lower ABEP than the AF relay. This is due to the reason that the RIS can effectively change the phase of reflected signals without buffering or processing the incoming signals, and the received signal quality can be enhanced by adjusting the phase shift of each element on the RIS.

VI. CONCLUSIONS

In this paper, we made a fair comparison between the IRS-aided and AF relay systems over mmWave channels. We first derived new statistical characterizations of the product of independent FTR RVs and the sum of product of FTR RVs, and used the results to obtain the exact PDF and CDF expressions of the RIS-aided system. In addition, the characterizations of end-to-end SNR of the AF relay system assuming either ideal or non-ideal hardware were obtained. We proposed a novel and simple way to obtain the optimal phases at the RIS, and we also proposed the optimal power allocation scheme for AF relay system. Then, the OP and the ABEP of two systems were presented to study their performances. In particular, our results show that when the transmit power is low, the threshold is high or the channel gain is high, the RIS-aided system can achieve the same performance as the AF relay system using a small number reflecting elements. Consequently, compared with the AF relay, RIS is of practical interest under mmWave communications.

APPENDIX A

PROOF OF THEOREM 2

1) *Proof of PDF:* The PDF of X can be formulated as [28, eq. (10)]

$$f_X(x) = \frac{1}{x} \frac{1}{2\pi i} \int_{\mathcal{L}} \mathbb{E}[X^s] x^{-s} ds \quad (\text{A-1})$$

where the integration path of \mathcal{L} goes from $\sigma - \infty j$ to $\sigma + \infty j$ and $\sigma \in \mathbb{R}$. To this effect, by inserting (7) into (A-1) and carrying out some algebraic manipulations, (A-1) can be rewritten as

$$f_X(x) = \frac{1}{x} \frac{1}{2\pi i} \prod_{\ell=1}^N \frac{m_\ell^{m_\ell}}{\Gamma(m_\ell)} \sum_{j_\ell=0}^{\infty} \frac{K_\ell^{j_\ell} d_{\ell j_\ell}}{j_\ell!} \frac{2}{\Gamma(j_\ell + 1)} \int_{\mathcal{L}} \prod_{\ell=1}^N \Gamma(1 + j_\ell + t) \left(x^2 \prod_{\ell=1}^N \left(\frac{1}{2\sigma_\ell^2} \right) \right)^{-t} dt. \quad (\text{A-2})$$

With the help of [13, eq. (9.301)], we can obtain (8).

2) *Proof of CDF:* The CDF of X can be expressed as

$$F_X(x) = \int_0^x f_r(r) dr. \quad (\text{A-3})$$

Substituting (8) into (A-3), we obtain

$$F_X(x) = \prod_{\ell=1}^N \frac{m_\ell^{m_\ell}}{\Gamma(m_\ell)} \sum_{j_\ell=0}^{\infty} \frac{K_\ell^{j_\ell} d_{\ell j_\ell}}{j_\ell!} \frac{2}{\Gamma(j_\ell + 1)} \int_0^x \frac{1}{t} G_{0,N}^{N,0} \left(t^2 \prod_{\ell=1}^N \left(\frac{1}{2\sigma_\ell^2} \right) \middle| \begin{matrix} - \\ 1 + j_1, \dots, 1 + j_N \end{matrix} \right) dt. \quad (\text{A-4})$$

Making the change of variable $t^2 = a$ and using [13, eq. (9.301)], we can rewrite (A-4) as

$$F_X(x) = \prod_{\ell=1}^N \frac{m_\ell^{m_\ell}}{\Gamma(m_\ell)} \sum_{j_\ell=0}^{\infty} \frac{K_\ell^{j_\ell} d_{\ell j_\ell}}{j_\ell!} \frac{1}{\Gamma(j_\ell + 1)} \frac{1}{2\pi i} \int_{\mathcal{L}} \prod_{\ell=1}^N \Gamma(1 + j_\ell + t) \left(\prod_{\ell=1}^N \left(\frac{1}{2\sigma_\ell^2} \right) \right)^{-t} I_{A_1} dt \quad (\text{A-5})$$

where

$$I_{A_1} = \int_0^{x^2} a^{-1-t} da = \frac{\Gamma(-t)}{\Gamma(1-t)} x^{-2t} \quad (\text{A-6})$$

where we have used [13, eq. (8.331.3)]. Substituting (A-6) into (A-5) and using [13, eq. (9.301)], we can obtain (9).

3) *Proof of MGF*: The generalized MGF of the product of FTR RVs can be obtained using

$$\mathcal{M}_X(s) = [e^{-xs}] = \int_0^\infty e^{-xs} f_X(x) dx. \quad (\text{A-7})$$

Substituting (8) into (A-7) and then using [13, eq. (9.301)], we can rewrite (A-7) as

$$\mathcal{M}_X(s) = \sum_{j_\ell=0}^{\infty} \prod_{\ell=1}^N \frac{K_\ell^{j_\ell} d_{\ell j_\ell}}{j_\ell!} \frac{m_\ell^{m_\ell}}{\Gamma(m_\ell)} \frac{2}{\Gamma(j_\ell + 1)} \frac{1}{2\pi i} \int_0^\infty x^{-1} e^{-xs} \int_{\mathcal{L}} \prod_{\ell=1}^N \Gamma(1 + j_\ell + t) \left(x^2 \prod_{\ell=1}^N \left(\frac{1}{2\sigma_\ell^2} \right) \right)^{-t} dt dx. \quad (\text{A-8})$$

According to Fubini's theorem, we can exchange the order of integrations in (A-8), and derive

$$\mathcal{M}_X(s) = \sum_{j_\ell=0}^{\infty} \prod_{\ell=1}^N \frac{K_\ell^{j_\ell} d_{\ell j_\ell}}{j_\ell!} \frac{m_\ell^{m_\ell}}{\Gamma(m_\ell)} \frac{2}{\Gamma(j_\ell + 1)} \frac{1}{2\pi i} \int_{\mathcal{L}} \prod_{\ell=1}^N \Gamma(1 + j_\ell + t) \left(\prod_{\ell=1}^N \left(\frac{1}{2\sigma_\ell^2} \right) \right)^{-t} I_{A_2} dt \quad (\text{A-9})$$

where

$$I_{A_2} = \int_0^\infty x^{-2t-1} e^{-xs} dx. \quad (\text{A-10})$$

With the help of [13, eq. (3.381.4)], I_{A_2} can be solved as

$$I_{A_2} = s^{2t} \Gamma(q - 2t). \quad (\text{A-11})$$

With the help of definition of Fox's H -function [14, eq. (1.2)] and substituting (A-11) into (A-9), we obtain (10) to complete the proof.

APPENDIX B

PROOF OF THEOREM 3

1) *Proof of PDF:* Let $\mathcal{M}_{X_\ell}(s)$ denote the MGF of the ℓ th product of two FTR RVs and we can derive the MGF of Z as

$$\mathcal{M}_Z(s) = \prod_{\ell=1}^L \mathcal{M}_{X_\ell}(s). \quad (\text{B-1})$$

Thus, the PDF of X can be expressed as

$$f_Z(z) = \mathcal{L}^{-1}[\mathcal{M}_X(s); z]. \quad (\text{B-2})$$

Substituting (10) into (B-2), after some algebraic manipulations, we have

$$f_Z(z) = \sum_{j_{1,1}, \dots, j_{L,1}=0}^{\infty} \cdots \sum_{j_{1,N}, \dots, j_{L,N}=0}^{\infty} \prod_{\ell=1}^L \prod_{\ell=1}^N \frac{K_{\ell,\ell}^{j_{\ell,\ell}} d_{\ell,\ell}^{j_{\ell,\ell}} m_{\ell,\ell}^{m_{\ell,\ell}}}{j_{\ell,\ell}! \Gamma(m_{\ell,\ell}) \Gamma(j_{\ell,\ell} + 1)} \frac{1}{I_{B_1}} \quad (\text{B-3})$$

where

$$\begin{aligned} I_{B_1} &= \mathcal{L}^{-1} \left[\left(\frac{1}{2\pi i} \right)^\ell \int_{\mathcal{L}_\ell} \prod_{\ell=1}^N \Gamma \left(1 + j_{\ell,\ell} + \frac{1}{2} s_\ell \right) \Gamma(-s_\ell) \left(s \prod_{\ell=1}^N (\sqrt{2} \sigma_{\ell,\ell}) \right)^{s_\ell} d s_\ell; z \right] \\ &= \frac{1}{2\pi i} \int_{\mathcal{L}} \left(\frac{1}{2\pi i} \right)^\ell \int_{\mathcal{L}_\ell} \prod_{\ell=1}^N \Gamma \left(1 + j_{\ell,\ell} + \frac{1}{2} s_\ell \right) \Gamma(-s_\ell) \left(s \prod_{\ell=1}^N (\sqrt{2} \sigma_{\ell,\ell}) \right)^{s_\ell} d s_\ell e^{sz} ds. \end{aligned} \quad (\text{B-4})$$

Note that the order of integration can be interchangeable according to Fubini's theorem, we can express

I_{B_1} as

$$I_{B_1} = \frac{1}{2\pi i} \left(\frac{1}{2\pi i} \right)^\ell \int_{\mathcal{L}_\ell} \prod_{\ell=1}^N \Gamma \left(1 + j_{\ell,\ell} + \frac{1}{2} s_\ell \right) \Gamma(-s_\ell) \left(\prod_{\ell=1}^N (\sqrt{2} \sigma_{\ell,\ell}) \right)^{s_\ell} I_{B_2} d s_\ell \quad (\text{B-5})$$

where

$$I_{B_2} = \int_{\mathcal{L}} s^{\sum_{\ell=1}^L s_\ell} e^{sz} ds. \quad (\text{B-6})$$

Let $sz = -b$ and we have

$$I_{B_2} = - \left(\frac{1}{z} \right)^{1 + \sum_{\ell=1}^L s_\ell} \int_{\mathcal{L}} (-b)^{\sum_{\ell=1}^L s_\ell} e^{-b} db. \quad (\text{B-7})$$

With the aid of [13, eq. (8.315.1)], I_{B_2} can be solved as

$$I_{B_2} = \left(\frac{1}{z} \right)^{1 + \sum_{\ell=1}^L s_\ell} \frac{2\pi i}{\Gamma \left(- \sum_{\ell=1}^L s_\ell \right)}. \quad (\text{B-8})$$

Combining (B-8), (B-5) and (B-3) and using the definition of the multivariate Fox's H -function [14, eq. (A-1)], we obtain (29) and complete the proof.

2) *Proof of CDF*: Following similar procedures as in Appendix B-1, we can derive the CDF of Z by taking the inverse Laplace transform of $Mz(s)/s$.

APPENDIX C

PROOF OF LEMMA 1

It is obvious that $F_{\gamma_{AF}}(z) = 0$ for $z < 0$ and $F_{\gamma_{AF}}(z) = 1$ for $z > 1/d$. Therefore, hereafter it is assumed that $0 \leq z \leq 1/d$. Let us define $U = c_2/\gamma_1$, $V = c_1/\gamma_2$ and $W = 1/\gamma_{AF} - d$. The PDF of W is obtained using the convolution theorem, namely

$$F_W(w) = \int_0^w F_U(w-x) f_V(x) dx. \quad (\text{C-1})$$

The CDFs of U and V can be expressed in terms of the CDFs of z_1 and z_2 , respectively, as

$$F_U(u) = 1 - F_{\gamma_1}\left(\frac{c_2}{u}\right), \quad f_V(v) = \frac{c_1}{v^2} f_{\gamma_2}\left(\frac{c_1}{v}\right). \quad (\text{C-2})$$

Thus, eq. (C-2) can be expressed as

$$F_W(w) = \int_0^w f_{\gamma_2}\left(\frac{c_1}{x}\right) \frac{c_1}{x^2} dx - \int_0^w F_{\gamma_1}\left(\frac{c_2}{w-x}\right) f_{\gamma_2}\left(\frac{c_1}{x}\right) \frac{c_1}{x^2} dx. \quad (\text{C-3})$$

By performing the change of variables $x = wt$, $F_W(w)$ can be further expressed as

$$F_W(w) = \int_0^1 f_{\gamma_2}\left(\frac{c_1}{wt}\right) \frac{c_1}{wt^2} dt - \int_0^1 F_{\gamma_1}\left(\frac{c_2}{w(1-t)}\right) f_{\gamma_2}\left(\frac{c_1}{wt}\right) \frac{c_1}{wt^2} dt. \quad (\text{C-4})$$

Noticing that $Z = \frac{1}{W+d}$ and employing a transformation of RVs, the CDF of γ_{AF} can be derived in terms of the CDF of W as

$$F_Z(z) = 1 - F_W\left(\frac{1}{z} - d\right). \quad (\text{C-5})$$

By using (C-5) and (C-4), after performing some mathematical manipulations, we obtain (26) and complete the proof.

APPENDIX D

PROOF OF THEOREM 4

1) *Proof of PDF*: Substituting (1) to (25) and after performing some straightforward manipulations, we obtain

$$f_{\gamma_{AF}}(z) = \frac{c_2 c_1 z}{(1-zd)^3} \sum_{j_1=0}^{\infty} \sum_{j_2=0}^{\infty} \prod_{\ell=1}^2 \left(\frac{m_{\ell}^{m_{\ell}} K_{\ell}^{j_{\ell}} d_{\ell}^{j_{\ell}} A_{\ell}^{j_{\ell}}}{\Gamma(m_{\ell}) j_{\ell}! 2\sigma_{\ell}^2 \Gamma(j_{\ell} + 1)} \right) I_{C_1} \quad (\text{D-1})$$

where

$$I_{C_1} = \int_0^1 \frac{1}{t^{2+j_1}} \frac{1}{(1-t)^{2+j_2}} \exp\left(-\frac{1}{2\sigma_1^2} \frac{c_2 z}{(1-zd)t}\right) \exp\left(-\frac{1}{2\sigma_2^2} \frac{c_1 z}{(1-zd)(1-t)}\right) dt. \quad (\text{D-2})$$

By using [29, eq. (01.03.07.0001.01)] and exchanging the order of integrations, I_{C_1} can be expressed as

$$I_{C_1} = \int_{\mathcal{L}_1} \int_{\mathcal{L}_2} \Gamma(s_1) \Gamma(s_2) \left(\frac{1}{2\sigma_1^2} \frac{c_2 z}{(1-zd)}\right)^{-s_1} \left(\frac{1}{2\sigma_2^2} \frac{c_1 z}{(1-zd)}\right)^{-s_2} I_{C_2} ds_2 ds_1 \quad (\text{D-3})$$

where

$$I_{C_2} = \int_0^1 \frac{1}{t^{2+j_1-s_1}} \frac{1}{(1-t)^{2+j_2-s_2}} dt. \quad (\text{D-4})$$

With the help of [13, eq. (3.251.1)] and [13, eq. (8.384.1)], I_{C_2} can be solved as

$$I_{C_2} = \frac{\Gamma(1-2-j_1+s_1) \Gamma(1-2-j_2+s_2)}{\Gamma(-2-j_2+s_2-j_1+s_1)}. \quad (\text{D-5})$$

Combining (D-5), (D-3) and using the definition of multivariate Fox's H -function [14, eq. (A-1)], we obtain (27) to complete the proof.

2) *Proof of CDF*: Substituting (1) and (2) to (26), we have

$$F_{\gamma_{AF}}(z) = 1 - F_1 + F_2 \quad (\text{D-6})$$

where

$$F_1 = \frac{z c_1}{(1-zd)} \frac{m_2^{m_2}}{\Gamma(m_2)} \sum_{j_2=0}^{\infty} \frac{K_2^{j_2} d_2^{j_2}}{j_2!} \frac{\left(\frac{z c_1}{(1-zd)}\right)^{j_2}}{\Gamma(j_2+1) (2\sigma_2^2)^{j_2+1}} \int_0^1 \frac{1}{t^{j_2}} \exp\left(-\frac{1}{2\sigma_2^2} \frac{z c_1}{(1-zd)t}\right) \frac{dt}{t^2}, \quad (\text{D-7})$$

$$F_2 = \frac{z c_1}{(1-zd)} \frac{m_1^{m_1}}{\Gamma(m_1)} \frac{m_2^{m_2}}{\Gamma(m_2)} \sum_{j_1=0}^{\infty} \sum_{j_2=0}^{\infty} \frac{K_1^{j_1} d_1^{j_1}}{j_1!} \frac{K_2^{j_2} d_2^{j_2}}{j_2!} \frac{1}{\Gamma(j_1+1) \Gamma(j_2+1) (2\sigma_2^2)^{j_2+1}} I_{C_3} \quad (\text{D-8})$$

where

$$I_{C_3} = \int_0^1 \frac{1}{t^{j_2+2}} \exp\left(-\frac{1}{2\sigma_2^2} \frac{zc_1}{(1-zd)t}\right) \gamma\left(j_1+1, \frac{1}{2\sigma_1^2} \frac{zc_2}{(1-zd)(1-t)}\right) dt. \quad (\text{D-9})$$

With the help of [13, eq. (3.381.8)], F_1 can be solved as

$$F_1 = \frac{m_2^{m_2}}{\Gamma(m_2)} \sum_{j_2=0}^{\infty} \frac{K_2^{j_2} d_2^{j_2}}{j_2!} \frac{1}{\Gamma(j_2+1)} \Gamma\left(1+j_2, \frac{1}{2\sigma_2^2} \frac{zc_1}{(1-zd)}\right). \quad (\text{D-10})$$

Using [29, eq. (01.03.07.0001.01)] and [29, eq. (06.06.07.0002.01)], we can express I_{C_3} as

$$I_{C_3} = \left(\frac{1}{2\pi i}\right)^2 \int_{\mathcal{L}_1} \int_{\mathcal{L}_2} \Gamma(s_2) \frac{\Gamma(s_1+j_1+1) \Gamma(-s_1)}{\Gamma(1-s_1)} \left(\frac{1}{2\sigma_2^2} \frac{zc_1}{(1-zd)}\right)^{-s_2} \left(\frac{1}{2\sigma_1^2} \frac{zc_2}{(1-zd)}\right)^{-s_1} I_{C_4} ds_2 ds_1 \quad (\text{D-11})$$

where

$$I_{C_4} = \int_0^1 \frac{1}{t^{j_2+2-s_2} (1-t)^{-s_1}} dt. \quad (\text{D-12})$$

With the help of [13, eq. (3.191.1)] and [13, eq. (8.384.1)], I_{C_4} can be derived as

$$I_{C_4} = \frac{\Gamma(1+s_1) \Gamma(s_2-j_2-1)}{\Gamma(s_1+s_2-j_2)}. \quad (\text{D-13})$$

Combining (D-13), (D-11), (D-8) and using the definition of multivariate Fox's H -function [14, eq. (A-1)], we obtain (28) and complete the proof.

REFERENCES

- [1] J. Zhang, E. Björnson, M. Matthaiou, D. W. K. Ng, H. Yang, and D. J. Love, "Multiple antenna technologies for beyond 5G," *arXiv:1910.00092*, 2019.
- [2] T. S. Rappaport, G. R. MacCartney, M. K. Samimi, and S. Sun, "Wideband millimeter-wave propagation measurements and channel models for future wireless communication system design," *IEEE Trans. Commun.*, vol. 63, no. 9, pp. 3029–3056, Sept. 2015.
- [3] J. M. Romero-Jerez, F. J. Lopez-Martinez, J. F. Paris, and A. J. Goldsmith, "The fluctuating two-ray fading model: Statistical characterization and performance analysis," *IEEE Trans. Wireless Commun.*, vol. 16, no. 7, pp. 4420–4432, Jul. 2017.
- [4] B. Rankov and A. Wittneben, "Spectral efficient protocols for half-duplex fading relay channels," *IEEE J. Sel. Areas Commun.*, vol. 25, no. 2, pp. 379–389, Feb. 2007.
- [5] T. J. Cui, M. Q. Qi, X. Wan, J. Zhao, and Q. Cheng, "Coding metamaterials, digital metamaterials and programmable metamaterials," *Light Sci. Appl.*, vol. 3, no. 10, pp. e218–e218, Oct. 2014.
- [6] C. Huang, A. Zappone, G. C. Alexandropoulos, M. Debbah, and C. Yuen, "Reconfigurable intelligent surfaces for energy efficiency in wireless communication," *IEEE Trans. Wireless Commun.*, vol. 18, no. 8, pp. 4157–4170, Aug. 2019.
- [7] E. Björnson, Ö. Özdogan, and E. G. Larsson, "Intelligent reflecting surface vs. decode-and-forward: How large surfaces are needed to beat relaying?" *IEEE Wireless Commun. Lett.*, vol. 9, no. 2, pp. 244–248, Feb. 2020.

- [8] M. O. Hasna and M.-S. Alouini, "Outage probability of multihop transmission over Nakagami fading channels," *IEEE Commun. Lett.*, vol. 7, no. 5, pp. 216–218, May 2003.
- [9] H. Shin and J. H. Lee, "Performance analysis of space-time block codes over keyhole Nakagami- m fading channels," *IEEE Trans. Veh. Technol.*, vol. 53, no. 2, pp. 351–362, Feb. 2004.
- [10] Y. Cui and H. Yin, "An efficient CSI acquisition method for intelligent reflecting surface-assisted mmWave networks," *arXiv:1912.12076*, 2019.
- [11] E. Bjornson, M. Matthaiou, and M. Debbah, "A new look at dual-hop relaying: Performance limits with hardware impairments," *IEEE Trans. Commun.*, vol. 61, no. 11, pp. 4512–4525, Nov. 2013.
- [12] J. Zhang, W. Zeng, X. Li, Q. Sun, and K. P. Peppas, "New results on the fluctuating two-ray model with arbitrary fading parameters and its applications," *IEEE Trans. Veh. Technol.*, vol. 67, no. 3, pp. 2766–2770, Mar. 2017.
- [13] I. S. Gradshteyn and I. M. Ryzhik, *Table of Integrals, Series, and Products*, 7th ed. Academic Press, 2007.
- [14] A. M. Mathai, R. K. Saxena, and H. J. Haubold, *The H-function: Theory and Applications*. Springer Science & Business Media, 2009.
- [15] O. S. Badarneh and D. B. da Costa, "Cascaded fluctuating two-ray fading channels," *IEEE Commun. Lett.*, vol. 23, no. 9, pp. 1497–1500, Sept. 2019.
- [16] K. P. Peppas, "A new formula for the average bit error probability of dual-hop amplify-and-forward relaying systems over generalized shadowed fading channels," *IEEE Wireless Commun. Lett.*, vol. 1, no. 2, pp. 85–88, Apr. 2012.
- [17] J. Sánchez, D. Osorio, E. Olivo, H. Alves, M. C. P. Paredes, and L. Urquiza-Aguiar, "On the statistics of the ratio of non-constrained arbitrary α - μ random variables: A general framework and applications," *arXiv:1902.07847*, Feb. 2019.
- [18] C. R. N. Da Silva, N. Simmons, E. J. Leonardo, S. L. Cotton, and M. D. Yacoub, "Ratio of two envelopes taken from $\alpha - \mu$, $\eta - \mu$, and $\kappa - \mu$ variates and some practical applications," *IEEE Access*, vol. 7, pp. 54 449–54 463, May 2019.
- [19] H. R. Alhennawi, M. M. El Ayadi, M. H. Ismail, and H.-A. M. Mourad, "Closed-form exact and asymptotic expressions for the symbol error rate and capacity of the h -function fading channel," *IEEE Trans. Veh. Technol.*, vol. 65, no. 4, pp. 1957–1974, Apr. 2015.
- [20] H. Chergui, M. Benjillali, and M.-S. Alouini, "Rician K -factor-based analysis of XLOS service probability in 5G outdoor ultra-dense networks," *IEEE Wireless Commun. Lett.*, vol. 8, no. 2, pp. 428–431, Apr. 2018.
- [21] Y. Han, W. Tang, S. Jin, C.-K. Wen, and X. Ma, "Large intelligent surface-assisted wireless communication exploiting statistical CSI," *IEEE Trans. Veh. Technol.*, vol. 68, no. 8, pp. 8238–8242, Aug. 2019.
- [22] G. P. Karatza, K. P. Peppas, N. C. Sagias, and G. V. Tsoulos, "Unified ergodic capacity expressions for AF dual-hop systems with hardware impairments," *IEEE Commun. Lett.*, vol. 23, no. 6, pp. 1057–1060, Jun. 2019.
- [23] M. O. Hasna and M. . Alouini, "Outage probability of multihop transmission over nakagami fading channels," *IEEE Commun. Lett.*, vol. 7, no. 5, pp. 216–218, May 2003.
- [24] Q. Wu and R. Zhang, "Beamforming optimization for intelligent reflecting surface with discrete phase shifts," in *Proc. IEEE ICASSP*, 2019, pp. 7830–7833.
- [25] E. Basar, M. Di Renzo, J. De Rosny, M. Debbah, M.-S. Alouini, and R. Zhang, "Wireless communications through reconfigurable intelligent surfaces," *IEEE Access*, vol. 7, pp. 116 753–116 773, Aug. 2019.
- [26] B. Allen and I. Munro, "Self-organizing binary search trees," *J. ACM*, vol. 25, no. 4, pp. 526–535, Apr. 1978.
- [27] I. Trigui, A. Laourine, S. Affes, and A. Stéphanne, "Performance analysis of mobile radio systems over composite fading/shadowing channels with co-located interference," *IEEE Trans. Wireless Commun.*, vol. 8, no. 7, pp. 3448–3453, Jul. 2009.
- [28] O. S. Badarneh, S. Muhaidat, P. C. Sofotasios, S. L. Cotton, K. Rabie, and D. B. da Costa, "The N *Fisher-snedecor \mathcal{F} cascaded fading model," in *Proc. WiMob*, Oct. 2018, pp. 1–7.
- [29] Wolfram, "The wolfram functions site," <http://functions.wolfram.com>.